

**Bulletin of the American Meteorological Society**  
**The California Baseline Ozone Transport Study (CABOTS)**  
 --Manuscript Draft--

<b>Manuscript Number:</b>	BAMS-D-18-0302
<b>Full Title:</b>	The California Baseline Ozone Transport Study (CABOTS)
<b>Article Type:</b>	Article
<b>Corresponding Author:</b>	Ian Faloon University of California Davis Davis, California UNITED STATES
<b>Corresponding Author's Institution:</b>	University of California Davis
<b>First Author:</b>	Ian Faloon
<b>Order of Authors:</b>	Ian Faloon Sen Chiao Arthur Eiserloh Andrew Langford Christoph Senff Raul Alvarez Guillaume Kirgis Dani Caputi Arthur Hu Laura Iraci Emma Yates Josette Marrero Ju-Mee Ryoo Stephen Conley Saffet Tanrikulu Jin Xu Toshihiro Kuwayama
<b>Manuscript Classifications:</b>	1.040: Complex terrain; 1.096: North America; 3.264: Mixing; 12.032: Air pollution; 12.036: Air quality; 12.116: Ozone
<b>Abstract:</b>	Ozone is one of the six 'criteria' pollutants identified by the U.S. Clean Air Act Amendment of 1970 as particularly harmful to human health. Concentrations have decreased markedly across the U.S. over the past 50 years in response to regulatory efforts, but continuing research on its deleterious effects have spurred further reductions in the legal threshold. The South Coast and San Joaquin Valley Air Basins of California remain the only two 'extreme' ozone non-attainment areas in the U.S. Further reductions of ozone in the West are complicated by significant background concentrations whose relative importance increases as domestic anthropogenic contributions decline and the national standards continue to be lowered. These background concentrations derive largely from uncontrollable sources including stratospheric intrusions, wildfires, and intercontinental transport. Taken together the exogenous sources complicate regulatory strategies and necessitate a much more precise understanding of the timing and magnitude of their contributions to regional air pollution. The California Baseline Ozone Transport Study was a field campaign coordinated across Northern/Central California during spring/summer 2016 aimed at observing daily variations in the ozone columns crossing the North American coastline, as well as the modification of the ozone layering downwind across the mountainous

	topography of California to better understand the impacts of background ozone on surface air quality in complex terrain.
<b>Author Comments:</b>	<p>Abstract:</p> <p>Ozone is one of the six 'criteria' pollutants identified by the U.S. Clean Air Act Amendment of 1970 as particularly harmful to human health. Concentrations have decreased markedly across the U.S. over the past 50 years in response to regulatory efforts, but continuing research on its deleterious effects have spurred further reductions in the legal threshold. The South Coast and San Joaquin Valley Air Basins of California remain the only two 'extreme' ozone non-attainment areas in the U.S. Further reductions of ozone in the West are complicated by significant background concentrations whose relative importance increases as domestic anthropogenic contributions decline and the national standards are lowered. These background concentrations derive largely from uncontrollable sources including stratospheric intrusions, wildfires, and intercontinental transport. Taken together these exogenous sources complicate regulatory strategies and a much more accurate apportionment of local contributions supplementing a complex background is critically needed. The California Baseline Ozone Transport Study was a field campaign coordinated across Northern/Central California during spring/summer 2016 aimed at observing daily variations in the ozone columns entering North American airspace, as well as their modification downwind across the complex topography of California to better understand the impacts of background ozone on surface air quality.</p>
<b>Suggested Reviewers:</b>	<p>Owen Cooper owen.r.cooper@noaa.gov Expert in this field, and did a lot of the work that motivated this project.</p> <p>Jerome Fast Jerome.Fast@pnnl.gov</p> <p>Alexander Gohm alexander.gohm@uibk.ac.at</p> <p>Tom Ryerson thomas.b.ryerson@noaa.gov</p> <p>Gail Tonnesen tonnesen.gail@epa.gov</p>

Post-Review Draft

1                                   **The California Baseline Ozone Transport Study (CABOTS)**

2    Ian C. Faloona<sup>1\*</sup>, Sen Chiao<sup>2</sup>, Arthur J. Eiserloh<sup>2</sup>, Raul J. Alvarez II<sup>3</sup>, Guillaume Kirgis<sup>4</sup>, Andrew O.  
3    Langford<sup>3</sup>, Christoph J. Senff<sup>4</sup>, Dani Caputi<sup>1</sup>, Arthur Hu<sup>1</sup>, Laura T. Iraci<sup>5</sup>, Emma L. Yates<sup>5</sup>, Josette  
4           E. Marrero<sup>5,9</sup>, Ju-Mee Ryoo<sup>5</sup>, Stephen Conley<sup>6</sup>, Saffet Tanrikulu<sup>7</sup>, Jin Xu<sup>8</sup>, and Toshihiro  
5                                   Kuwayama<sup>8</sup>

6                                   <sup>1</sup>University of California, Davis, California

7                                   <sup>2</sup> San José State University, California

8                                   <sup>3</sup>NOAA/ESRL/Chemical Sciences Division, Boulder, Colorado

9                                   <sup>4</sup>CIRES and NOAA/ESRL/Chemical Sciences Division, Boulder, Colorado

10                                  <sup>5</sup>NASA Ames Research Center, Moffett Field, California

11                                  <sup>6</sup>Scientific Aviation, Inc., Boulder, Colorado

12                                  <sup>7</sup>BAAQMD, San Francisco, California

13                                  <sup>8</sup>California Air Resources Board, Sacramento, California

14                                  <sup>9</sup>Now at Sonoma Technology, Petaluma, California

15

16    **Capsule Summary:** A coordinated field campaign across Northern and Central California during  
17    the spring and summer of 2016 measured daily fluctuations in the ozone column flowing onshore  
18    as well as its modification by regional emissions during transport over land, and helps to clarify  
19    the impacts that the variable chemical boundary conditions have on surface air quality in complex  
20    terrain.

21    \*Corresponding Author: Ian Faloona (icfaloona@ucdavis.edu)

22 **Abstract**

23 Ozone is one of the six 'criteria' pollutants identified by the U.S. Clean Air Act Amendment of  
24 1970 as particularly harmful to human health. Concentrations have decreased markedly across  
25 the U.S. over the past 50 years in response to regulatory efforts, but continuing research on its  
26 deleterious effects have spurred further reductions in the legal threshold. The South Coast and  
27 San Joaquin Valley Air Basins of California remain the only two 'extreme' ozone non-attainment  
28 areas in the U.S. Further reductions of ozone in the West are complicated by significant  
29 background concentrations whose relative importance increases as domestic anthropogenic  
30 contributions decline and the national standards continue to be lowered. These background  
31 concentrations derive largely from uncontrollable sources including stratospheric intrusions,  
32 wildfires, and intercontinental transport. Taken together the exogenous sources complicate  
33 regulatory strategies and necessitate a much more precise understanding of the timing and  
34 magnitude of their contributions to regional air pollution. The California Baseline Ozone  
35 Transport Study was a field campaign coordinated across Northern/Central California during  
36 spring/summer 2016 aimed at observing daily variations in the ozone columns crossing the North  
37 American coastline, as well as the modification of the ozone layering downwind across the  
38 mountainous topography of California to better understand the impacts of background ozone on  
39 surface air quality in complex terrain.

40

41

42 Air pollution is responsible for over 6 million premature deaths annually worldwide –twice as  
43 many as AIDS, malaria, and tuberculosis combined (Landrigan et al. 2018). It is estimated that air  
44 pollution directly contributes to more than 200,000 premature deaths per year in the U.S.  
45 (Caiazzo et al. 2013). Many of these deaths are linked to fine particulate matter (PM), but ozone  
46 ( $O_3$ ) plays a central role in most air quality issues because it is the principal source of hydroxyl  
47 (OH) and nitrate ( $NO_3$ ) radicals, the leading agents of atmospheric oxidation, which produce PM  
48 and other components of photochemical smog. Moreover, tropospheric ozone is an important  
49 greenhouse gas with a radiative forcing of  $0.4 (\pm 0.12) \text{ Wm}^{-2}$ , just shy of methane ( $CH_4$ ) (Myhre et  
50 al. 2013) and is a phytotoxic pollutant that impacts agricultural yields and tree growth (Lapina et  
51 al. 2016). Long-term exposure to  $O_3$  has been implicated in the development of asthma in  
52 children (McConnell et al. 2002) and reduced cognitive performance in the elderly (Zhang et al.  
53 2018).

54 Tropospheric ozone originates from both natural and anthropogenic sources and is  
55 photochemically produced by the auto-catalytic oxidation of carbon monoxide (CO) and volatile  
56 organic compounds (VOCs) in the presence of nitrogen oxides ( $NO_x \equiv NO + NO_2$ .) Natural sources  
57 include direct injection from the stratosphere and secondary production from emissions of non-  
58 anthropogenic origins such as biogenic VOCs (BVOC) emitted by vegetation (Sindelarova et al.  
59 2014), and  $NO_x$  from unmanaged soils (Vinken et al. 2014) and lightning (Zhang et al. 2003).  
60 Wildfires (see sidebar) are another growing source of both  $NO_x$  and VOCs (Andreae and Merlet  
61 2001; Jaffe and Wigder 2012). Because the principal loss of ozone requires photolysis followed  
62 by reaction with water vapor, and water vapor mixing ratios decrease dramatically with height  
63 due to the Clausius-Clapeyron relation, the photochemical lifetime of ozone is altitude

64 dependent and ranges from one week in the marine boundary layer (Conley et al. 2011) to one  
65 year in the upper troposphere (Kley et al. 1996). With a global average lifetime of about 3 weeks  
66 (Young et al. 2013), the ozone observed directly upwind of the U.S. West Coast can therefore  
67 include anthropogenic contributions transported from East Asia and Europe, and even ozone that  
68 originated in the U.S. but has circumnavigated the globe. This so-called 'baseline' ozone  
69 constitutes a significant fraction of the ambient concentrations measured in the Western U.S.  
70 Here we conform to the definition proposed by the Task Force on Hemispheric Transport of Air  
71 Pollution (HTAP) and adopted in the recent review by Jaffe et al. (2018): "Baseline ozone is  
72 defined as the observed ozone at a site when it is not influenced by recent, locally emitted or  
73 anthropogenically produced pollution (HTAP 2010)." 'Background' ozone, on the other hand  
74 (including, for example, North American Background, or Policy Relevant Background), is a model  
75 estimate of the O<sub>3</sub> abundances calculated when the anthropogenic precursor emissions from  
76 specific areas are omitted or "zeroed out". Throughout this work we will use the term 'baseline'  
77 due to the observational emphasis of the study.

78 The Western U.S. is particularly susceptible to transported ozone because of several physical  
79 factors. First, the baroclinicity induced by the North American coastline at the end of the North  
80 Pacific storm track, coupled with the planetary wave activity of the adjacent cordillera promotes  
81 cross-tropopause transport of stratospheric ozone in this region (Sprenger and Wernli 2003). This  
82 process peaks in the spring but can occur throughout the year (Škerlak et al. 2014). Second,  
83 synoptic-scale subsidence in the lee of the Pacific subtropical anticyclone draws both naturally  
84 occurring ozone and transported pollution (including ozone and its precursors such as  
85 peroxyacetyl nitrate, PAN) from the middle and upper troposphere towards the surface (Hudman

86 et al. 2004). And third, the deep convective atmospheric boundary layers (ABLs) of the interior  
87 West provide stronger coupling between the free troposphere (FT) and the surface (Langford et  
88 al. 2017). This direct convective entrainment is strongest during the summer months above arid  
89 and/or high elevation surfaces but is weaker within California's Central Valley where the  
90 unusually shallow ABLs are deepest in the springtime (Bianco et al. 2011) and decrease markedly  
91 during summer as a result of mesoscale subsidence induced by the mountain-valley circulation  
92 (TrousdeLL et al., 2016) and irrigation practices (Li et al. 2016).

93 Several modeling studies (Brown-Steiner and Hess 2011; Liang et al. 2004) have shown that  
94 the trans-Pacific transport of anthropogenic ozone from Asia is fundamentally different in spring  
95 and summer. Episodic long-range transport from Asia increases in frequency with altitude, and  
96 peaks in the late spring (April-June) when the prevailing westerlies are strong and extratropical  
97 cyclone activity is highest (Lin et al. 2012a). During the summer, much of the Asian pollution is  
98 lofted into the upper troposphere (>5 km) by deep convection associated with the East Asian  
99 summer monsoon. This summertime ozone is then transported eastward by the prevailing  
100 westerly winds aloft, often remaining well above the Coast Range and the Sierra Nevada;  
101 however, some is brought downward in the quasi-isentropic flow equatorward and toward the  
102 elevated diabatic heating of the mountains.

103 Despite an estimated reduction in anthropogenic ozone enhancements above baseline levels  
104 by a factor of 5 since 1980 (Parrish et al. 2017), California and other western states must continue  
105 to achieve significant new emission controls on ozone precursors in order to attain compliance  
106 with the current National Ambient Air Quality Standard (NAAQS). In light of observations  
107 indicating rising emissions of ozone precursors from Asia (Sun et al. 2018; Verstraeten et al.

108 2015), more frequent wild fires (Westerling et al. 2006), and a possible increase in stratosphere-  
109 troposphere exchange (Stevenson et al. 2006), concern is mounting about the ability of California  
110 and other western states to meet the NAAQS because of a rising baseline component beyond  
111 their regional or national regulatory purview.

112 Numerous modeling (Jacob et al. 1999; Lin et al. 2012b; Pfister et al. 2011) and measurement  
113 (Cooper et al. 2011; Jaffe et al. 1999; Parrish et al. 2014; Yates et al. 2017) studies have examined  
114 the impact of baseline ozone on surface concentrations across California, but there remains a  
115 great deal of uncertainty about the contributions of stratospheric and other transported ozone  
116 to surface concentrations in the San Joaquin Valley (SJV), the southern part of the California  
117 Central Valley and one of only two 'extreme' ozone non-attainment areas remaining in the U.S.  
118 (U.S. EPA Green Book, <https://www.epa.gov/green-book>). Much of this uncertainty is thought to  
119 result from a lack of detailed information about the vertical distribution of ozone. Intermittent  
120 measurements by ozonesondes or aircraft do not provide the temporal coverage needed to easily  
121 evaluate how well models can determine the fraction of baseline ozone contributing to surface  
122 concentrations measured in the SJV, and this deficiency is by no means limited to California. The  
123 main objective of the California Baseline Ozone Transport Study (CABOTS) was to observe the  
124 daily changes in ozone layering at the coast (approximately upwind of California) and  
125 simultaneously the layering in the Central Valley (downwind of the major emission sources and  
126 coastal mountains) in order to produce an unprecedented data set that might serve to promote  
127 ensuing modeling studies. Some issues that the novel data set may help to illuminate include: i.)  
128 the fidelity with which air quality models represent ozone transport on synoptic, regional, and  
129 local scales in complex terrain; ii.) the relative contributions of stratosphere-troposphere



130 exchange, Asian emissions, and wildfires to the abundances and variability observed in the ozone  
131 profiles in and around California; and iii.) the extent to which exogenous ozone that has been  
132 transported from afar mixes down to surface sites affecting ozone NAAQS violations in the SJV.  
133 Because the project was sponsored primarily by the California Air Resources Board (CARB), a state  
134 agency, its initial scope is more limited than many federal scale projects in that it did not include  
135 observations of a large suite of photochemical reactants nor did it sponsor extensive modeling  
136 efforts. This work summarizes the measurements and unique meteorology of California that  
137 serve as the context for this novel data set and attempts to draw attention to its potential utility  
138 for future modeling studies of the impacts of long-range transport on global air quality issues.

139

## 140 **THE CABOTS FIELD CAMPAIGN.**

### 141 *Geography*

142 The San Joaquin Valley encompasses the southern two-thirds (~65,000 km<sup>2</sup>) of the 700 km  
143 long Central Valley of California (Figure 1). Although it is one of the largest valleys in the world,  
144 the geometry and meteorology are not too dissimilar from other places such as the Po Valley in  
145 Italy, the San Luis Valley in Southern Colorado, the Latrobe Valley in Australia, and the Central  
146 Valley of Chile. The 50 – 100 km wide San Joaquin Valley is bounded by the Southern Coast Ranges  
147 with elevations of less than 1.5 km above mean sea level (asl) to the west, the Sierra Nevada (<4  
148 km asl) to the east, and the San Emigdio and Tehachapi Mountains (<2.5 km asl) to the south.  
149 The flat valley floor rises gradually from sea level in the Sacramento–San Joaquin River Delta near  
150 Stockton to ~130 m asl at Bakersfield to the south (see Figure 1). The SJV is one of the most

151 important agricultural areas in the U.S. responsible for 12% of all U.S. agricultural production and  
152 home to about 10% of California's residents.

### 153 *Measurement Suite*

154 Measurements of ozone vertical profiles by ozonesondes, a ground-based lidar, and aircraft,  
155 together with surface ozone concentrations were made from May to August of 2016 (Table 1,  
156 Figure 2). The core measurements included near-daily ozonesonde profiles collected at two sites  
157 along the coast and an ozone lidar data set collected in Visalia, a city of nearly 140,000 residents  
158 located deep within the San Joaquin Valley, approximately 60 km southeast of Fresno. Figure 2  
159 shows the locations of the two primary CABOTS ground sites: the ozonesonde launch site at the  
160 University of California, Davis Bodega Marine Laboratory (UCD BML) in Bodega Bay (BBY) and the  
161 lidar site at the Visalia Municipal Airport (VMA) on the eastern side of the SJV. The UCD BML  
162 (38.319°N, 123.072°W) is located approximately 80 km north of San Francisco and ozonesondes  
163 were launched daily there 6 days per week from the middle of May to the middle of August 2016  
164 by researchers from San José State University (SJSU). Additionally, a second launch site was  
165 operated at the same periodicity for a subset of the project at Half Moon Bay (HMB, 37.504°N,  
166 122.483°W) located 25 km to the south of San Francisco.

167 The National Oceanic and Atmospheric Administration (NOAA) TOPAZ (Tunable Optical  
168 Profiler for Aerosols and oZone) differential absorption lidar (DIAL) system (Alvarez et al. 2011)  
169 was operated daily during two 3-week long intensive operating periods: IOP1 (May 27-June 18)  
170 and IOP2 (July 18-August 7). TOPAZ uses a scanning mirror for measurements at different  
171 elevation angles to provide quasi-continuous ozone and aerosol backscatter profiles from 25 m

172 to about 6 km above ground level ( $\geq 8$  km at night). A radar wind profiler and radio-acoustic  
173 sounding system (RASS) at the Visalia airport provided measurements of virtual temperature  
174 profiles up to 1-1.5 km and winds up to 4 km.

175 In addition to these core measurements, the University of California, Davis (UCD) and  
176 Scientific Aviation, Inc. team conducted aircraft measurements to characterize the evolution of  
177 ozone layering in the lower atmosphere ( $< 1,500$  m) over the course of the entire diurnal cycle  
178 from Fresno to Bakersfield. Flights for this separate study investigating the effects of residual  
179 layer ozone and its mixing on surface exceedances overlapped with some of the CABOTS project.  
180 Additionally, supplemental funding was provided by the US EPA to study the afternoon ABL and  
181 photochemical ozone production rates in the valley between Fresno and Visalia, upwind of the  
182 TOPAZ lidar, on six additional days: July 27-29 and August 4-6 (Trousdel et al. 2019).  
183 Furthermore, the Alpha Jet Atmospheric eXperiment (AJAX) of the NASA Ames Research Center  
184 (Hamill et al. 2016) performs regular missions to measure ozone and greenhouse gases, such as  
185 ozone, carbon dioxide ( $\text{CO}_2$ ), methane ( $\text{CH}_4$ ), and formaldehyde (HCHO) over California and  
186 Nevada, and was coordinated to contribute to CABOTS. A comprehensive intercomparison of the  
187 TOPAZ lidar with both airborne platforms (Langford et al. 2019) found excellent agreement  
188 (within 5 ppbv on average) among the three measurements.

189 In addition to the usual ozone data collected at nearly 80 CARB (25 in the SJV Air Basin)  
190 routine surface sites in Central and Northern California that are available for the study  
191 (<https://www.arb.ca.gov/aqmis2/aqdselect.php>), the San Joaquin Valley Air Pollution Control  
192 District (SJVAPCD) had funded ozone measurements made by UC Davis at the Oliver Observing  
193 Station (<http://tycho.mira.org/oosweather/>), which is operated by the Monterey Institute for

194 Research in Astronomy (MIRA: <http://www.mira.org/>) on Chews Ridge. This solar and wind-  
195 powered mountain observatory is at an elevation of 1,550 m asl in the Los Padres National Forest  
196 40 km southeast of Monterey but located about half that distance downwind from the Big Sur  
197 coastline to the southwest from whence the winds blow two-thirds of the time (Asher et al.,  
198 2018). Measurements of O<sub>3</sub>, NO, NO<sub>2</sub> and NO<sub>x</sub> collected at this site during CABOTS are available  
199 although much of it was heavily impacted by the Soberanes Fire during the second IOP, which  
200 burned along the northwest perimeter of the Oliver Observing Station from late July to early  
201 October.

202 *Synoptic Setting*

203 The SJV has a Mediterranean climate well-suited for agricultural production. The winters are  
204 usually cool and moist, but the summers are hot and dry with less than 5% of the annual  
205 precipitation falling between May and September ([https://cdec.water.ca.gov/snow\\_rain.html](https://cdec.water.ca.gov/snow_rain.html)).  
206 The principal ABL summer wind patterns are dominated by the thermally-driven mesoscale  
207 circulations of the coupled sea-land/valley-mountain flow. Onshore winds can usually only  
208 penetrate into California's Central Valley at breaks in the Coast Range because the marine ABL  
209 tends to be well below the height of the coastal mountains (Dorman et al., 2000), and mostly the  
210 winds feed in through the Carquinez Strait east of the San Francisco Bay Area (Figure 1). This  
211 inflow is modulated by the synoptic conditions as well as diurnal up-valley winds and by  
212 upslope/downslope flow along the flanks of the Sierra Nevada and Coastal Ranges (Bao et al.  
213 2008; Zhong et al. 2004). The northwesterly inflow brings ozone and other pollutants from the  
214 San Francisco Bay area and Sacramento (Fast et al. 2012) up the valley towards Bakersfield, but  
215 also flushes the valley with clean marine air, particularly at night when up-valley winds can

216 strengthen into an elevated low-level jet (LLJ) (Caputi et al. 2019). Some of this flow exits the  
217 valley through the Tehachapi Pass 75 km southeast of Bakersfield, but much is blocked by the  
218 mountains and recirculated northward where it interacts with cross-valley drainage flows and  
219 the LLJ to form an early morning low-level counterclockwise circulation known as the Fresno eddy  
220 (Bao et al. 2008; Lin and Jao 1995), which is believed to foster the buildup of ozone in the SJV  
221 (Beaver and Palazoglu 2009).

222 The daytime upslope winds carry ozone and other pollutants from the SJV into the  
223 surrounding mountains (Panek et al. 2013) with the circulation closed by elevated compensation  
224 flows above the valley (Zardi and Whiteman 2013). Subsidence created by this mountain-valley  
225 circulation and the synoptically persistent North Pacific High (TrousdeU et al. 2016), and to a  
226 lesser extent, evaporative cooling associated with widespread agricultural irrigation (Li et al.  
227 2016), limits the growth of the convective mixed layers (ML) in the central SJV to ~1 km or less  
228 during summer (Bianco et al. 2011) with somewhat deeper mixed layers in the southern part of  
229 the valley where the converging up-valley flow is lifted by the weir of the Tehachapi Mountains  
230 (TrousdeU et al. 2016). The sidewall venting creates elevated pollution layers above the ML that  
231 spread across the valley when the synoptic forcing is weak (Fast et al. 2012; Leukauf et al., 2016).  
232 Ozone remaining in the residual layer left after the ML decays can be re-entrained the following  
233 day or turbulently mixed into the stable nocturnal boundary layer by the LLJ and destroyed at the  
234 surface (Caputi et al. 2019). Above the average daytime ABL height (500 – 600 m), there exists an  
235 intermediate layer, composed of a mixture of free tropospheric inflow coming over the coast  
236 range and air lofted above the ABL by the sidewall slope flows. Because this region is a mixture  
237 of baseline FT air and surface-influenced ABL air, and because it is stably stratified yet

238 intermittently turbulent (Faloona 2018) we refer to it as a buffer layer (BuL) similar to that  
239 described by Russell et al. (1998) over the ocean.

240 The synoptic and mesoscale subsidence associated with the Pacific High and mountain-valley  
241 circulation also inhibits cloud formation during the summer, and the combination of high  
242 temperatures and clear skies in July and August fosters rapid photochemical production of O<sub>3</sub>  
243 from NO<sub>x</sub> and VOC precursors transported into the valley by the northwesterly inflow, emitted  
244 by urban sources, or released by distributed transportation, agricultural, and petrochemical  
245 sources within the SJV (TrousdeLL et al., 2019; Pusede et al. 2014). To some degree the Fresno  
246 Eddy recirculates these pollutants within the Southern SJV to help create an ozone hotspot near  
247 Fresno (Beaver and Palazoglu 2009), although the strong associated low-level jet may also induce  
248 vertical mixing at night that depletes ozone (Caputi et al. 2019).

249 Synoptic charts of reanalysis data for both TOPAZ IOPs, as well as a June – August average for  
250 2010-2015, are shown in Figure 3 (data from the National Center for Environmental Prediction’s  
251 North American Regional Reanalysis, NCEP/NARR: [https://www.esrl.noaa.gov/psd/cgi-  
252 bin/data/narr/plotday.pl](https://www.esrl.noaa.gov/psd/cgi-bin/data/narr/plotday.pl)). On the 900 hPa (≈ 1 km asl) geopotential height fields, the synoptic  
253 patterns for both IOPs are seen to closely resemble the climatological pattern, with a thermal  
254 low over the southern California/Nevada border and alongshore, equatorward winds over the  
255 ocean. A mean up-valley (northwesterly) flow is present in the SJV due to the mountain-valley  
256 circulation, but is geostrophically reinforced by the pressure gradient between the offshore  
257 Pacific High and inland thermal low.

258 Figure 4 shows the monthly average tropospheric column ozone concentrations derived from  
259 the difference between the total column ozone measured by the NASA Aura Ozone Monitoring  
260 Instrument (OMI) and the stratospheric column measurements made by the Aura Microwave  
261 Limb Sounder (MLS) (Ziemke et al. 2006) during the three core months of the CABOTS project.  
262 Superimposed on the tropospheric averaged concentrations are the NCEP reanalysis winds at the  
263 300 hPa isobaric level for each month considering that the main summertime trans-Pacific  
264 transport is centered aloft near 8 km (Brown-Steiner and Hess 2011). The patches of elevated  
265 ozone over the central Pacific in June and the faster winds may represent the trailing edge of  
266 springtime baroclinicity in the midlatitudes which is often accompanied by enhanced  
267 stratosphere-troposphere exchange. The seasonal progression of Figure 4 also shows the  
268 poleward advancement of the ITCZ with its depleted ozone and easterly winds that shunt the  
269 main Asian effluent northward throughout the summer season. Interannual variations in this  
270 advancement associated with the Pacific Decadal Oscillation (PDO) have been shown to markedly  
271 influence the long-term trends in ozone observed at the baseline site on Mauna Loa, Hawaii (Lin  
272 et al. 2014).

273 **Some Examples of the CABOTS measurements**

274 The curtain plot of Figure 5 shows the daily ozonesonde data from both the Bodega and Half  
275 Moon Bay sites. The daily data exhibits patterns similar to those seen in the Trinidad Head  
276 analyses of less frequent (weekly) soundings over a decade reported by Oltmans et al. (2008),  
277 with undulations of ozone concentrations in the mid-to-upper troposphere of 3-5 week  
278 periodicities. A comparable ozonesonde study by Cooper et al. (2011) coordinated with the  
279 CalNex campaign (Ryerson et al. 2013) reported the ozone percentile distributions observed in

280 near daily profiles above Trinidad Head (THD, 320 km north along the coast from Bodega Bay) for  
281 5 weeks (May 10- June 19) during 2010. At 2 km the percentiles at 5%, 33%, 50%, 67%, and 95%  
282 were found to be 30, 44, 47, 51, and 62 ppbv (their Figure 10). Figure 5 shows three or four  
283 episodes of enhanced ozone in the upper troposphere at BBY and the depletion of marine ABL  
284 ozone, below about 500 m, as the summer progresses due to photochemical destruction in a  
285 more or less pristine environment. The observed day-to-day variability does appear to be larger  
286 during the three-month interval of CABOTS which shows the percentile values of 5%, 33%, 50%,  
287 67%, and 95% at 2 km to be 36, 51, 57, 62, and 77 ppbv. The 10 ppbv greater median ozone at 2  
288 km above BBY than at THD is consistent with the upward sloping meridional isopleths reported  
289 in Cooper et al. (2011). The larger interquartile range may be due to the longer interval of the  
290 CABOTS data set, but is indicative that day-to-day variability is important for accurately  
291 constraining the oxidant boundary conditions along the North American inflow. In order to take  
292 a preliminary look at how well a commonly used chemical transport model captures the ozone  
293 amounts and variability as a chemical boundary condition, a comparison of the observed mean  
294 and standard deviation profiles (black) with those generated in the Model for Ozone and Related  
295 Chemical Tracers (MOZART, Emmons et al., 2010) (red) is shown in Figure 6 for the 24  
296 ozonesondes launched between mid-July and mid-August at the HMB site. While the model does  
297 capture the strong gradients at the top of the marine ABL well, there does seem to be a  
298 systematic 5-15 ppbv underestimate throughout most of the troposphere followed by  
299 overpredictions greater than 20 ppbv above 10 km (not shown). It is also important to note that  
300 in the region between 1-3 km, which likely influences the surface ozone levels in the interior  
301 Central Valley and western face of the Sierras the most, the observed daily standard deviation is



302 ~60% greater than is captured in the model. Furthermore, in agreement with the findings  
303 presented in Figure 6 of frequent ozone concentrations well above 60-70 ppb (mean + 1 standard  
304 deviation) at 1.5 km altitudes and above, an analysis of the ozone time series collected at Chews  
305 Ridge from 2012-2014 determined that the ODV for this remote site located in a National Forest  
306 in the coastal mountains was 70.5 ppbv, technically in violation of the NAAQS.

307 Figure 7 shows the compiled time series from the TOPAZ ozone lidar at Visalia over the course  
308 of the two IOPs. The scalloped appearance of the daily curtain plots is caused by increased solar  
309 background radiation near local noon, which reduces the lidar maximum range. In general, the  
310 lidar data shows the rich textures of the air above the valley with frequent episodes of high ozone  
311 advected overhead in the upper troposphere (also seen in Figure 5), as well as synoptic  
312 accumulations of ozone in the ABL, but also in the buffer layer above up to 2-2.5 km. Generally,  
313 the features appear to slope downward over the course of several days as would be expected  
314 with isentropic (westerly) flow over the heated (and better mixed) continental atmosphere.

315 The TOPAZ measurements from IOP2 are also presented as diurnally-averaged profiles in  
316 Figure 8. Only the diurnal hours with more than 5 days of measurements are shown. The statistics  
317 are most robust for the hours between 1300 and 1900 PDT when more than 12 days of  
318 measurements are averaged. The corresponding mean winds from the co-located SJVAPCD  
319 profiler are superimposed on each plot; wind speeds less than  $2 \text{ ms}^{-1}$  are represented by crosses.  
320 The wind vectors show the horizontal wind direction with the top of the plot representing north  
321 and the right side east (arrows that point to the right in the figure therefore represent *westerly*  
322 winds.) The mean winds, primarily northwesterly throughout a deep layer (ABL + BuL) during  
323 daytime, begin westerly (upslope) in the late morning and grow stronger and more northerly in

324 the afternoon ABL as the up-valley thermal circulation prevails. The general pattern appears very  
325 similar to those shown in Zhong et al. (2004) and Bao et al. (2008) that were based on data  
326 collected at Visalia during the 2000 Central California Ozone Study. The solid black line in each  
327 plot represents the ABL height calculated from gradients in the RASS virtual temperature profiles.  
328 The dashed line in Figure 8 shows the ABL height calculated from direct measurements of the  
329 vertical velocity variance by an experimental NOAA ESRL Doppler lidar deployed next to TOPAZ  
330 during the last two weeks of the campaign. These two independent measurements are in very  
331 good agreement and are also consistent with the gradients observed in the TOPAZ UV backscatter  
332 profiles. All three methods indicate that the mean ABL height of ~500 m at Visalia corresponds  
333 fairly well to the reported average afternoon ABL heights of 550 m for the region between Visalia  
334 and Fresno (Trousdel et al., 2019) during the six EPA flights of the Scientific Aviation Mooney.  
335 The diurnally-averaged O<sub>3</sub> data for IOP2 shows depletion overnight in a shallow nocturnal  
336 boundary layer due to nitrate production and dry deposition (Caputi et al. 2019) followed by a  
337 well-mixed buildup of O<sub>3</sub> in the ABL during the day. The prevalence of elevated ozone (>70 ppb,  
338 orange colors) between 500 – 2,500 m in these average profiles of Figure 8 is evidence that ABL  
339 air is lofted into the buffer layer above due to daytime slope flow along the flanks of the valley  
340 during its up-valley progression towards the southeast. Further evidence of this slope venting is  
341 presented for other scalars in the discussion surrounding Figure 10 that follows. Note that this  
342 buffer layer lies above any residual layer left behind when the convective mixed layer decays in  
343 the evening. The accumulation of afternoon lofting is especially evident in Figure 8 at 21:00.

344 Another representation of the three-layered valley atmosphere is illustrated in Figure 9,  
345 which shows a terrain cross-section running from the coast near Chews Ridge perpendicular to

346 the valley axis into the Sierra Nevada (topography data from the NASA Shuttle Radar Tomography  
347 Mission.) Winds from the Half Moon Bay ozonesondes are plotted along the coast, and those  
348 averaged from the Visalia RASS from 12:00-16:00 July – August at the corresponding cross-valley  
349 axis distance. Vector averaged winds are represented by the arrows (north oriented toward the  
350 top of the page), and scalar average wind speeds are displayed by the arrow color. The red and  
351 the blue lines are average potential temperature and ozone, respectively, measured by the  
352 Mooney aircraft during the 6 EPA flights. These data show an average ABL height of ~600 m  
353 wherein the afternoon ozone tends to be the highest, and then distinctly show an intermediate,  
354 statically-stable BuL where the ozone concentrations are somewhere between ABL and free  
355 tropospheric (above ~2,000 m) amounts. These data show the typical southwesterly flow at  
356 Chews Ridge entering the valley over the coastal ridgeline, but as the air travels inland it is swept  
357 up into the up-valley (northwesterly) wind of the SJV that dominates from the surface all the way  
358 to the top of the buffer layer. Somewhere between 2,000 – 2,500 m the vector wind average is  
359 almost the null vector, a near balance of up- and down-valley winds, with an average scalar wind  
360 speed near  $4\text{-}5\text{ ms}^{-1}$ , similar to the onshore flow at the same level. Thus, the presence of the high  
361 southern Sierra Nevada downwind appears to block the flow's progression, but does not stagnate  
362 as much as recirculate the air within the valley buffer layer. Higher up, in the free troposphere,  
363 the obstruction of the mountains also impedes the flow, weakening the Coriolis force, but above  
364 the reach of the mountain-valley thermal circulation air is pushed down the background pressure  
365 gradient (Figure 3), which is directed more or less down-valley, driving southeasterly winds aloft.  
366 Note that despite the well-defined thermodynamic capping inversion atop the valley boundary

367 layer, there is little wind shear across the inversion as the daytime up-valley flow persists  
368 throughout the ABL and BuL.

369 A more instantaneous picture of the valley atmosphere's layering can be seen in Figure 10  
370 showing NASA AJAX spiral/vertical profile at the coastal BBY site (dark purple) compared to the  
371 inland profile flown near Visalia (cyan) only 30 minutes later on June 15. Because the AJAX flight  
372 was scheduled for the morning, the ozonesonde was launched at BBY early to be nearly  
373 coincident at 10:00 PDT. The five scalars shown (from left to right: CO<sub>2</sub>, CH<sub>4</sub>, O<sub>3</sub>, H<sub>2</sub>O, and HCHO)  
374 clearly indicate the difference between the baseline composition of the air moving onshore at  
375 the coast and the air heavily influenced by California's Central Valley. In this instance, the ABL at  
376 Visalia appears to be around 800 m and the buffer layer seems to extend up to about 2,500 m.  
377 The long chemical lifetime and strong surface sources of CH<sub>4</sub> from agriculture and oil production  
378 in the SJV (Trousdel et al. 2016) clearly show the layering of an ABL with methane enhanced by  
379 100-150 ppbv over the baseline observed offshore. The secondary enhancements of CH<sub>4</sub> at 1,500  
380 m and 2,300 m clearly show the lofting of ABL valley air into the buffer layer that had occurred  
381 most likely on the previous afternoon when western slope sidewall venting is most active (Fast  
382 et al., 2012; Leukauf et al., 2016), injecting these two layers that wind up over Visalia on the  
383 morning of June 15. These layers are more pronounced in CO<sub>2</sub> where they are characterized by  
384 drawdown from the agricultural photosynthesis of the valley environment, far more prevalent  
385 than where the particular CH<sub>4</sub> sources may have been. At the lowest levels, just above the Visalia  
386 airport and CA-99, the CO<sub>2</sub> signal exceeds the marine baseline due to fossil fuel combustion.  
387 HCHO also exhibits lofted plumes at 1,500 and 2,300 m over Visalia, similar to methane. Because  
388 the midday lifetime of HCHO due to photolysis and reaction with OH is only about 3 hr (Choi et

389 al. 2010), yet should be very long in the dark away from the surface, the presence of significant  
390 amounts of HCHO (up to 1.5 ppbv) shows that the lofting into the buffer layer is accomplished  
391 on the time scale of several hours over the course of any day.

392 The June 15 vertical profile measurements can be put into a larger perspective. Figure 11  
393 superimposes the AJAX CH<sub>4</sub> and O<sub>3</sub> profiles at Visalia from Figure 10 on the TOPAZ time-height  
394 aerosol and ozone curtain plots, respectively. The curtain plots show relatively elevated O<sub>3</sub>  
395 extending up to ~2,700 m in the BuL. Different origins for these layers is consistent with the  
396 abrupt wind shift around 1.5 km. The buffer layer is capped by very clean air with less than 30  
397 ppbv of O<sub>3</sub> and low aerosol backscatter. The absence of turbulence in this layer is reflected by  
398 the rapid loss in the wind profiler return signals, and veering of the winds to westerly flow,  
399 consistent with the climatological pressure field presented in Figure 3, at the bottom of the clean  
400 layer (FT) can be seen. Above lies a 2 km thick layer with >80 ppbv of O<sub>3</sub> (and low aerosol)  
401 consistent with transported Asian pollution. The superimposed AJAX profile in Figure 11 shows  
402 that the aircraft sampled the very bottom of the transported pollution layer (not shown here, but  
403 exhibiting enhanced CO<sub>2</sub>, HCHO, and CH<sub>4</sub>) before descending into the clean layer.

404 Because CABOTS obtained many different vertical profiles of ozone across the state it is  
405 possible to look at how lower tropospheric ozone layers correlate across large distances. As  
406 Parrish et al. (2010) point out, ozonesonde measurements aloft may correlate with various  
407 surface sites downwind in a wide lateral swath not due to direct parcel trajectories, but because  
408 ozone laminae that are commonly found in the lower troposphere often extend for hundreds of  
409 kilometers in the horizontal (Liu et al. 2009). Figure 12 shows the correlations between the two  
410 coastal ozonesonde sites 100 km apart for the 22 days with simultaneous launches. The layers

411 seem to be spatially large enough to encompass both locations at altitudes between 1.5-2 km  
412 (near the altitude of the Chews Ridge observations), 4 km, and up near 6 km, with correlation  
413 coefficients of about 0.8 (the solid circles in Figure 12 represent the correlations with p-values  
414 less than 0.05.) The blue line of the left graph in Figure 12 shows the correlations between the  
415 BBY ozonesondes and the fixed Chews Ridge measurements at the same hour 260 km south along  
416 the coast (the correlation coefficient is calculated between the surface measurement and each  
417 altitude bin of the ozonesonde and lidar). Here the observations at the mountain top site are  
418 influenced by dry deposition to the forests and experience some influences of the continental  
419 sources, but there is still a correlation of nearly 0.4 with air sampled between 0.8-1.2 km above  
420 Bodega Bay. The correlation between the mountain site at Chews Ridge and the Visalia lidar  
421 inland shows a pronounced peak just below 2.5 km (green dashed line, right axis) and supports  
422 the idea that the Chews Ridge observatory may serve as a decent monitor of the inflow air over  
423 the coast range that dilutes the ABL air that is lofted into the buffer layer over the SJV. And finally,  
424 the measurements that were taken the farthest apart, 400 km between BBY and Visalia, show  
425 some modest correlations at 4.5 km and 1 km (red line, right panel.) The latter correlation near  
426 0.5 corroborates the FLEXPART modeling results of Cooper et al. (2011) showing a strong  
427 influence of air parcels at 1 km above Pt. Reyes (~30 km south along the coast from BBY) and  
428 their receptor region covering the 'south central' SJV in dictating that flow above the marine ABL  
429 gets drawn into the sea/valley breeze circulation that affects the flow up to about 2 km in the  
430 valley.

#### 431 **Summary**

432 The collective observations of 440 hours of O<sub>3</sub> lidar profiles over Visalia, over 100 coastal  
433 ozonesondes, and several targeted airborne surveys acquired during the 3-month CABOTS field  
434 experiment have the potential to greatly illuminate the meteorological mechanisms that  
435 determine the vertical distribution of O<sub>3</sub> above the central San Joaquin Valley. The high temporal  
436 resolution (daily for the coastal ozonesondes and daytime hourly for the lidar in the Central  
437 Valley) data set should be able to provide novel constraints on modeling efforts, ultimately  
438 producing new insights into the transport and mixing processes contributing to the high surface  
439 O<sub>3</sub> levels found in this and other large valleys around the world. The lidar, RASS, and airborne  
440 measurements all confirmed the unusually shallow convective mixed layers of the SJV and the  
441 formation of a persistent buffer layer above the ABL between about 0.5 and 2.5 km. Because of  
442 the surrounding topography the buffer layer overlying the well-mixed boundary layer is made up  
443 of partially stagnating air polluted by regional surface sources and a continuous dilution of  
444 incoming free tropospheric air that contains a highly variable amount of exogenous ozone usually  
445 present in discrete layers.

446 The TOPAZ lidar also frequently detected elevated O<sub>3</sub> layers between 4 and 6 km above the  
447 valley floor consistent with biomass burning, transport from Asia, or descent from the lower  
448 stratosphere. Many of these layers most likely passed over the Sierra Nevada into the  
449 Intermountain West where they may have been entrained by the much deeper convective mixed  
450 layers that form in that hot, dry higher elevation region (Langford et al. 2015; Langford et al.  
451 2018).

452 The high frequency daily ozonesondes showed a dramatic gradient in ozone reaching the  
453 coast from a median of 23 ppbv near the ocean surface and rising rapidly on average 17 ppb km<sup>-1</sup>

454 <sup>1</sup> up to 2 km, consistent with rapid photochemical destruction in the summertime marine  
455 boundary layer. Above that strong gradient the average rise is an order of magnitude gentler  
456 (about 2 ppb km<sup>-1</sup>), however the standard deviation increases aloft. The daily ozonesondes at  
457 Bodega Bay discovered the appearance of ozone concentrations below 3 km exceeding 70 ppbv,  
458 the 8 hr ambient air quality standard, on average once every 5 days. Initial comparisons with a  
459 chemical transport model commonly used to provide the chemical boundary conditions at the  
460 North American coast indicate a low bias of about 10 ppbv in the lowest 3 km, below which the  
461 air flow damns up along the western edge of the Southern Sierra Nevada mountains and  
462 potentially influences surface concentrations in California. The project data set was fortunate to  
463 observe the coastal and valley air during several weeks of the Soberanes Fire, a large wildfire that  
464 burned 130,000 acres in the coastal mountains over the course of nearly 3 months. The detailed  
465 observations of ozone in the complex terrain of the western US is publicly available (at  
466 <https://www.esrl.noaa.gov/csd/groups/csd3/measurements/cabots/>) and may serve to  
467 challenge future modeling efforts that attempt to quantify the episodic trans-Pacific transport  
468 and impact of distant ozone sources on ongoing surface air quality violations in the mountainous  
469 west.

470

471 **Acknowledgements**

472 The California Baseline Ozone Transport Study (CABOTS) field measurements described here  
473 were funded by the California Air Resources Board (CARB) under contracts #15RD007 (San José  
474 State University), #15RD012 (NOAA ESRL), #14-308 (UC Davis), and #17RD004 (NASA Ames). We  
475 would like to thank Jin Xu and Eileen McCauley of CARB for their support and assistance in the



476 planning and execution of the project, and are grateful to the CARB and the San Joaquin Valley  
477 Unified Air Pollution Control District (SJVAPCD) personnel who provided logistical support during  
478 the execution of the field campaign. We would also like to thank Cathy Burgdorf-Rasco of NOAA  
479 ESRL and CIRES for maintaining the CABOTS data site. The NOAA team would also like to thank  
480 Ann Weickmann, Scott Sandberg, and Richard Marchbanks for their assistance during the field  
481 campaign. The NOAA/ESRL lidar operations were also supported by the NOAA Climate Program  
482 Office, Atmospheric Chemistry, Carbon Cycle, and Climate (AC4) Program and the NASA-  
483 sponsored Tropospheric Ozone Lidar Network (TOLNet, [http://www-  
484 air.larc.nasa.gov/missions/TOLNet/](http://www-air.larc.nasa.gov/missions/TOLNet/)). The UC Davis/Scientific Aviation measurements were also  
485 supported by the U.S. Environmental Protection Agency and Bay Area Air Quality Management  
486 District through contract #2016-129. I.C.F. was also supported by the California Agricultural  
487 Experiment Station, Hatch project CA-D-LAW-2229-H. The NASA AJAX project was also supported  
488 with Ames Research Center Director's funds, and the support and partnership of H211, LLC is  
489 gratefully acknowledged. J.E.M. and J.-M.R. were supported through the NASA Postdoctoral  
490 Program. The CABOTS data are archived at <https://www.esrl.noaa.gov/csd/projects/cabots/>.  
491

492 **SIDEBAR 1: Regulatory History of O<sub>3</sub> NAAQS and California standards**

493 Exposure to ozone (O<sub>3</sub>) can trigger a variety of health problems, including decreased lung  
494 function and pulmonary inflammation, especially for children, elderly, and those with pre-  
495 existing health conditions such as asthma (EPA 2013). To protect human health, the first ambient  
496 air quality standards (AAQS) in California were set by the Department of Public Health (DPH) in  
497 1959, which set one-hour 0.15 parts-per-million (ppm) limit for photochemical oxidant levels in  
498 outdoor air. In 1967, the California Air Resources Board (CARB) was established and was granted  
499 authority to set future AAQS for the state. The federal Clean Air Act (CAA) of 1970 established  
500 the National Ambient Air Quality Standards (NAAQS), which set thresholds for criteria air  
501 pollutant levels in outdoor air (EPA 1970). Ground-level O<sub>3</sub> is categorized as one of the six criteria  
502 air pollutants regulated under NAAQS. Since then, California has continued to invest and lead a  
503 multitude of air quality and health research projects, including the evaluation of the peer-  
504 reviewed scientific literature on health effects of exposure. These activities led to the adoption  
505 of new O<sub>3</sub> standards, including the one-hour 0.09 ppm O<sub>3</sub> standard in 1988 when O<sub>3</sub> was  
506 identified as the primary link to respiratory health problems within the group of oxidants present  
507 in the atmosphere. This was also the year when the state legislature adopted the California CAA  
508 with strategies that include transportation emission control measures. Following the evaluation  
509 mandated by the Children’s Environmental Health Protection Act of 1999, CARB and Office of  
510 Environmental Health Hazard Assessment (OEHHA) recommended a new 0.070 ppm O<sub>3</sub> standard  
511 for the maximum daily 8-hr ozone average (MDA8) in 2005 based on human health and  
512 environmental impact assessments on O<sub>3</sub>. In October 2015, U.S. EPA followed suit and adopted  
513 the 0.070 ppm threshold for the 8-hour O<sub>3</sub> NAAQS. Compliance with the NAAQS is determined

514 by the “ozone design value” or ODV, the 3-year running average of the fourth highest MDA8  
515 ozone concentration observed each year at a given site. The ODV is a metric of the high end of  
516 the ozone distribution and roughly equivalent to the upper 98th percentile. Non-attainment  
517 areas must develop a State Implementation Plan (SIP) that demonstrates how new controls will  
518 reduce ground-level ozone to levels below the latest health-based standard. As a result of such  
519 continued efforts to minimize the adverse effects of O<sub>3</sub>, the maximum eight-hour O<sub>3</sub>  
520 concentration in the South Coast Air Basin (one of the most polluted regions in California), is now  
521 a factor of three lower despite a threefold increase in the number of passenger cars on the road,  
522 doubling of population, and economic growth of over two times.

523

524 **SIDEBAR 2: Do wildfires influence O<sub>3</sub>, where and by how much?**

525 Fires generate smoke (fine particulates or PM<sub>2.5</sub>) and a variety of gaseous compounds,  
526 including NO<sub>x</sub> and VOCs, the photochemical precursors of O<sub>3</sub>. The net production of O<sub>3</sub> by  
527 wildfires is highly variable, however, with many contradictory observations reported in the  
528 literature (Jaffe and Wigder 2012). The NO<sub>x</sub> and VOC emission rates depend on many factors  
529 including fuel type and combustion temperature, and the subsequent production of O<sub>3</sub> depends  
530 on the plume injection height, smoke density, and cloud cover. The amount of O<sub>3</sub> within a given  
531 smoke plume also varies with distance from the fire. Measurements made near active fires  
532 sometimes show a decrease in O<sub>3</sub> relative to baseline concentrations because of titration by NO  
533 (and possibly reduced NO<sub>2</sub> photolysis rates in the shade of the smoke plume), and measurements  
534 made far downwind often show little additional O<sub>3</sub> production if the NO<sub>x</sub> has been depleted or  
535 sequestered into more stable compounds like peroxyacetyl nitrate (PAN). The >132,000 acre

536 Soberanes Fire was the largest wildfire in California during 2016. The National Interagency Fire  
537 Center estimated it to be at the time the most expensive wildland fire in U.S. history with  
538 suppression costs exceeding \$262 million. The fire was started on the morning of July 22 by an  
539 illegal campfire in Garrapata State Park on the windward side of the coast range along California's  
540 Big Sur coast. It spread southeast from there over the next 10 weeks and by mid-August was  
541 burning along the perimeter of the Oliver Observing Station at Chews Ridge (Figure SB2.1). The  
542 fire burned more than 57,500 acres (40% of the final burn area) during the first two weeks, and  
543 smoke from the fire filled much of the central SJV by the last week of July when the highest  
544 surface ozone values of 2016 were recorded.

545 **References**

546 Alvarez, R. J., II, and Coauthors, 2011: Development and Application of a Compact, Tunable, Solid-  
547 State Airborne Ozone Lidar System for Boundary Layer Profiling, *J. Atmos. Ocean Tech.*, **28**,  
548 1258-1272, 10.1175/Jtech-D-10-05044.1.

549 Andreae, M. O., and P. Merlet, 2001: Emission of trace gases and aerosols from biomass burning.  
550 *Global Biogeochemical Cycles*, **15**, 955-966.

551 Asher, E. C., and Coauthors, 2018: The Transport of Asian Dust and Combustion Aerosols and  
552 Associated Ozone to North America as Observed From a Mountaintop Monitoring Site in the  
553 California Coast Range. *Journal of Geophysical Research: Atmospheres*, **123**, 5667-5680.

554 Bao, J. W., S. A. Michelson, P. O. G. Persson, I. V. Djalalova, and J. M. Wilczak, 2008: Observed  
555 and WRF-simulated low-level winds in a high-ozone episode during the Central California  
556 Ozone Study. *Journal of Applied Meteorology and Climatology*, **47**, 2372-2394.

557 Beaver, S., and A. Palazoglu, 2009: Influence of synoptic and mesoscale meteorology on ozone  
558 pollution potential for San Joaquin Valley of California. *Atmospheric Environment*, **43**, 1779-  
559 1788.

560 Bianco, L., I. V. Djalalova, C. W. King, and J. M. Wilczak, 2011: Diurnal Evolution and Annual  
561 Variability of Boundary-Layer Height and Its Correlation to Other Meteorological Variables  
562 in California's Central Valley. *Bound-Lay Meteorol*, **140**, 491-511.

563 Brown-Steiner, B., and P. Hess, 2011: Asian influence on surface ozone in the United States: A  
564 comparison of chemistry, seasonality, and transport mechanisms. *Journal of Geophysical  
565 Research-Atmospheres*, **116**.

566 Caiazzo, F., A. Ashok, I. A. Waitz, S. H. L. Yim, and S. R. H. Barrett, 2013: Air pollution and early  
567 deaths in the United States. Part I: Quantifying the impact of major sectors in 2005.  
568 *Atmospheric Environment*, **79**, 198-208.

569 Caputi, D. J., I. Faloona, J. Trousdell, J. Smoot, N. Falk, and S. Conley, 2019: Residual layer ozone,  
570 mixing, and the nocturnal jet in California's San Joaquin Valley. *Atmospheric Chemistry and*  
571 *Physics*, **19**, 4721-4740.

572 CARB, 2005: History of Ozone an Oxidant Ambient Air Quality Standards. May 6, 2006 ed.,  
573 California Air Resources Board.

574 Choi, W., and Coauthors, 2010: Observations of elevated formaldehyde over a forest canopy  
575 suggest missing sources from rapid oxidation of arboreal hydrocarbons. *Atmospheric*  
576 *Chemistry and Physics*, **10**, 8761-8781.

577 Conley, S. A., I. C. Faloona, D. H. Lenschow, A. Karion, and C. Sweeney, 2014: A Low-Cost System  
578 for Measuring Horizontal Winds from Single-Engine Aircraft. *J. Atmos. Ocean. Technol.*, **31**,  
579 1312-1320.

580 Conley, S. A., and Coauthors, 2011: A complete dynamical ozone budget measured in the tropical  
581 marine boundary layer during PASE. *Journal of Atmospheric Chemistry*, **68**, 55-70.

582 Cooper, O. R., and Coauthors, 2011: Measurement of western U.S. baseline ozone from the  
583 surface to the tropopause and assessment of downwind impact regions. *Journal of*  
584 *Geophysical Research-Atmospheres*, **116**, doi:10.1029/2011JD016095.

585 Doorman, C.E., T. Holt, D.P. Rogers, and K. Edwards, 2000: Large-scale structure of the June–July  
586 1996 marine boundary layer along California and Oregon. *Monthly Weather Review*, **128**,  
587 1632-1652.

588 Emmons, L. K., et al. (2010a), Description and evaluation of the Model for Ozone and Related  
589 chemical Tracers, version 4 (MOZART-4), *Geosci. Model Dev.*, 3, 43–67.

590 EPA: Summary of the Clean Air Act 42 U.S.C. §7401 et seq. (1970). [Available online at  
591 <https://www.epa.gov/laws-regulations/summary-clean-air-act.>]

592 —, 2013: Integrated Science Assessment (ISA) of Ozone (O<sub>3</sub>) and Related Photochemical  
593 Oxidants. Feb 2013 ed., EPA.

594 Ewing, S. A., J. N. Christensen, S. T. Brown, R. A. Vancuren, S. S. Cliff, and D. J. Depaolo, 2010: Pb  
595 isotopes as an indicator of the Asian contribution to particulate air pollution in urban  
596 California. *Environmental Science & Technology*, **44**, 8911-8916.

597 Faloon, I., 2018: Ozone in the Lower Atmosphere and its Contribution to High Ozone  
598 Concentrations at Ground-Level in the Southern San Joaquin Valley.

599 Fast, J. D., and Coauthors, 2012: Transport and mixing patterns over Central California during the  
600 carbonaceous aerosol and radiative effects study (CARES). *Atmospheric Chemistry and*  
601 *Physics*, **12**, 1759-1783.

602 Hamill, P., L. T. Iraci, E. L. Yates, W. Gore, T. P. Bui, T. Tanaka, and M. Loewenstein, 2016: A New  
603 Instrumented Airborne Platform for Atmospheric Research. *B Am Meteorol Soc*, **97**, 397-404.

604 HTAP, T., 2010: *Hemispheric Transport of Air Pollution, Part A: Ozone and Particulate Matter*.  
605 United Nations Publications.

606 Hudman, R. C., and Coauthors, 2004: Ozone production in transpacific Asian pollution plumes  
607 and implications for ozone air quality in California. *Journal of Geophysical Research-*  
608 *Atmospheres*, **109**.

609 Jacob, D. J., J. A. Logan, and P. P. Murti, 1999: Effect of rising Asian emissions on surface ozone  
610 in the United States. *Geophysical Research Letters*, **26**, 2175-2178.

611 Jaffe, D. A., and N. L. Wigder, 2012: Ozone production from wildfires: A critical review.  
612 *Atmospheric Environment*, **51**, 1-10.

613 Jaffe, D. A., and Coauthors, 2018: Scientific assessment of background ozone over the U.S.:  
614 Implications for air quality management. *Elem Sci Anth.*, **6**.

615 Jaffe, D. A., and Coauthors, 1999: Transport of Asian air pollution to North America. *Geophysical*  
616 *Research Letters*, **26**, 711-714.

617 Kley, D., P. Crutzen, H. Smit, H. Vömel, S. Oltmans, H. Grassl, and V. Ramanathan, 1996:  
618 Observations of near-zero ozone concentrations over the convective Pacific: Effects on air  
619 chemistry. *Science*, **274**, 230-233.

620 Landrigan, P. J., and Coauthors, 2018: The *Lancet* Commission on pollution and  
621 health. *The Lancet*, **391**, 462-512.



622 Langford, A. O., and Coauthors, 2015: An overview of the 2013 Las Vegas Ozone Study (LVOS):  
623 Impact of stratospheric intrusions and long-range transport on surface air quality.  
624 *Atmospheric Environment*, **109**, 305-322.

625 Langford, A. O., and Coauthors, 2017: Entrainment of stratospheric air and Asian pollution by the  
626 convective boundary layer in the southwestern U.S. *Journal of Geophysical Research:*  
627 *Atmospheres*, **122**, 1312-1337.

628 Langford, A. O., and Coauthors, 2018: Coordinated profiling of stratospheric intrusions and  
629 transported pollution by the Tropospheric Ozone Lidar Network (TOLNet) and NASA Alpha  
630 Jet Atmospheric eXperiment (AJAX): Observations and comparison to HYSPLIT, RAQMS, and  
631 FLEXPART. *Atmospheric Environment*, **174**, 1-14.

632 Langford, A. O., and Coauthors, 2019: Intercomparison of lidar, aircraft, and surface ozone  
633 measurements in the San Joaquin Valley during the California Baseline Ozone Transport  
634 Study (CABOTS). *Atmos. Meas. Tech.*, **12**, 1889-1904.

635 Lapina, K., D. K. Henze, J. B. Milford, and K. Travis, 2016: Impacts of foreign, domestic, and state-  
636 level emissions on ozone-induced vegetation loss in the United States. *Environmental*  
637 *Science & Technology*, **50**, 806-813.

638 Leukauf, D., A. Gohm, and M.W. Rotach, 2016: Quantifying horizontal and vertical tracer mass  
639 fluxes in an idealized valley during daytime. *Atmospheric Chemistry and Physics*, **16**, 20,  
640 13,049-13,066.

641 Li, J., A. Mahalov, and P. Hyde, 2016: Impacts of agricultural irrigation on ozone concentrations  
642 in the Central Valley of California and in the contiguous United States based on WRF-Chem  
643 simulations. *Agricultural and Forest Meteorology*, **221**, 34-49.

644 Liang, Q., L. Jaeglé, D. A. Jaffe, P. Weiss-Penzias, A. Heckman, and J. A. Snow, 2004: Long-range  
645 transport of Asian pollution to the northeast Pacific: Seasonal variations and transport  
646 pathways of carbon monoxide. *Journal of Geophysical Research: Atmospheres*, **109**.

647 Lin, M. Y., L. W. Horowitz, S. J. Oltmans, A. M. Fiore, and S. M. Fan, 2014: Tropospheric ozone  
648 trends at Mauna Loa Observatory tied to decadal climate variability. *Nat Geosci*, **7**, 136-143.

649 Lin, M. Y., and Coauthors, 2012a: Springtime high surface ozone events over the western United  
650 States: Quantifying the role of stratospheric intrusions. *Journal of Geophysical Research-*  
651 *Atmospheres*, **117**, D00v22.

652 Lin, M. Y., and Coauthors, 2012b: Transport of Asian ozone pollution into surface air over the  
653 western United States in spring. *Journal of Geophysical Research-Atmospheres*, **117**, D00v07.

654 Lin, Y. L., and I. C. Jao, 1995: A Numerical Study of Flow Circulations in the Central Valley of  
655 California and Formation Mechanisms of the Fresno Eddy. *Monthly Weather Review*, **123**,  
656 3227-3239.

657 Liu, G. P., D. W. Tarasick, V. E. Fioletov, C. E. Sioris, and Y. J. Rochon, 2009: Ozone correlation  
658 lengths and measurement uncertainties from analysis of historical ozonesonde data in North  
659 America and Europe. *Journal of Geophysical Research-Atmospheres*, **114**.

660 McConnell, R., and Coauthors, 2002: Asthma in exercising children exposed to ozone: a cohort  
661 study. *The Lancet*, **359**, 386-391.

662 Myhre, G., and Coauthors, 2013: Anthropogenic and natural radiative forcing. *Climate change*,  
663 **423**, 658-740.

664 Oltmans, S. J., A. S. Lefohn, J. M. Harris, and D. S. Shadwick, 2008: Background ozone levels of air  
665 entering the west coast of the US and assessment of longer-term changes. *Atmospheric*  
666 *Environment*, **42**, 6020-6038.

667 Panek, J., D. Saah, A. Esperanza, A. Bytnerowicz, W. Fraczek, and R. Cisneros, 2013: Ozone  
668 distribution in remote ecologically vulnerable terrain of the southern Sierra Nevada, CA.  
669 *Environ Pollut*, **182**, 343-356.

670 Parrish, D. D., L. M. Young, M. H. Newman, K. C. Aikin, and T. B. Ryerson, 2017: Ozone Design  
671 Values in Southern California's Air Basins: Temporal Evolution and US Background  
672 Contribution. *Journal of Geophysical Research-Atmospheres*, **122**, 11166-11182.

673 Parrish, D. D., K. C. Aikin, S. J. Oltmans, B. J. Johnson, M. Ives, and C. Sweeny, 2010: Impact of  
674 transported background ozone inflow on summertime air quality in a California ozone  
675 exceedance area. *Atmospheric Chemistry and Physics*, **10**, 10093-10109.

676 Parrish, D. D., and Coauthors, 2014: Long-term changes in lower tropospheric baseline ozone  
677 concentrations: Comparing chemistry-climate models and observations at northern  
678 midlatitudes. *Journal of Geophysical Research: Atmospheres*, **119**, 5719-5736.

679 Pfister, G. G., and Coauthors, 2011: Characterizing summertime chemical boundary conditions  
680 for air masses entering the US West Coast. *Atmospheric Chemistry and Physics*, **11**, 1769-  
681 1790.

682 Pierce, R., and Coauthors, 2003: Regional Air Quality Modeling System (RAQMS) predictions of  
683 the tropospheric ozone budget over east Asia. *Journal of Geophysical Research:*  
684 *Atmospheres*, **108**.

685 Pierce, R. B., and Coauthors, 2007: Chemical data assimilation estimates of continental US ozone  
686 and nitrogen budgets during the Intercontinental Chemical Transport Experiment–North  
687 America. *Journal of Geophysical Research: Atmospheres*, **112**.

688 Pusede, S. E., and Coauthors, 2014: On the temperature dependence of organic reactivity,  
689 nitrogen oxides, ozone production, and the impact of emission controls in San Joaquin  
690 Valley, California. *Atmospheric Chemistry and Physics*, **14**, 3373-3395.

691 Russell, L. M., and Coauthors, 1998: Bidirectional mixing in an ACE 1 marine boundary layer  
692 overlain by a second turbulent layer. *Journal of Geophysical Research-Atmospheres*, **103**,  
693 16411-16432.

694 Ryerson, T. B., and Coauthors, 2013: The 2010 California Research at the Nexus of Air Quality and  
695 Climate Change (CalNex) field study. *Journal of Geophysical Research-Atmospheres*, **118**,  
696 5830-5866.

697 Sindelarova, K., and Coauthors, 2014: Global data set of biogenic VOC emissions calculated by  
698 the MEGAN model over the last 30 years. *Atmospheric Chemistry and Physics*, **14**, 9317-9341.

699 Singh, H. B., C. Cai, A. Kaduwela, A. Weinheimer, and A. Wisthaler, 2012: Interactions of fire  
700 emissions and urban pollution over California: Ozone formation and air quality simulations.  
701 *Atmospheric Environment*, **56**, 45-51.

702 Škerlak, B., M. Sprenger, and H. Wernli, 2014: A global climatology of stratosphere–troposphere  
703 exchange using the ERA-Interim data set from 1979 to 2011. *Atmospheric Chemistry and*  
704 *Physics*, **14**, 913–937.

705 Sprenger, M., and H. Wernli, 2003: A northern hemisphere climatology of cross-tropopause  
706 exchange for the ERA15 time period (1979–1993). *Journal of Geophysical Research-*  
707 *Atmospheres*, **108**, doi:10.1029/2002JD002636.

708 Stevenson, D. S., and Coauthors, 2006: Multimodel ensemble simulations of present-day and  
709 near-future tropospheric ozone. *Journal of Geophysical Research: Atmospheres*, **111**.

710 St Clair, J. M, Swanson, A. K, Bailey, S. A., Wolfe, G. M., Marrero, J. E., Iraci, L. T., Hagopian, J. G.,  
711 Hanisco, T. F., 2017: A new non-resonant laser-induced fluorescence instrument for the  
712 airborne in situ measurement of formaldehyde. *Atmospheric Measurement Techniques*, **10**,  
713 **12**, 4833–4844.

714 Sun, W., M. Shao, C. Granier, Y. Liu, C. S. Ye, and J. Y. Zheng, 2018: Long-Term Trends of  
715 Anthropogenic SO<sub>2</sub>, NO<sub>x</sub>, CO, and NMVOCs Emissions in China. *Earth's Future*, **6**, 1112–1133.

716 Trousdell, J. F., S. A. Conley, A. Post, and I. C. Faloona, 2016: Observing entrainment mixing,  
717 photochemical ozone production, and regional methane emissions by aircraft using a simple  
718 mixed-layer framework. *Atmospheric Chemistry and Physics*, **16**, 15433–15450.

719 Trousdell, J. F., D. Caputi, J. Smoot, S. A. Conley, and I. C. Faloona, 2019: Photochemical  
720 Production of Ozone and Emissions of NO<sub>x</sub> and CH<sub>4</sub> in the San Joaquin Valley. *Atmos. Chem.*  
721 *Phys.*, **19**, 10697–10716.

722 Verstraeten, W. W., J. L. Neu, J. E. Williams, K. W. Bowman, J. R. Worden, and K. F. Boersma,  
723 2015: Rapid increases in tropospheric ozone production and export from China. *Nat. Geosci.*,  
724 **8**, 690-+.

725 Vinken, G. C. M., K. F. Boersma, J. D. Maasackers, M. Adon, and R. V. Martin, 2014: Worldwide  
726 biogenic soil NO<sub>x</sub> emissions inferred from OMI NO<sub>2</sub> observations.  
727 *Atmospheric Chemistry and Physics*, **14**, 10363-10381.

728 Westerling, A. L., H. G. Hidalgo, D. R. Cayan, and T. W. Swetnam, 2006: Warming and earlier  
729 spring increase western US forest wildfire activity. *science*, **313**, 940-943.

730 Yates, E. L., and Coauthors, 2017: An Assessment of Ground Level and Free Tropospheric Ozone  
731 Over California and Nevada. *Journal of Geophysical Research-Atmospheres*, **122**, 10089-  
732 10102.

733 Young, P. J., and Coauthors, 2013: Pre-industrial to end 21st century projections of tropospheric  
734 ozone from the Atmospheric Chemistry and Climate Model Intercomparison Project  
735 (ACCMIP). *Atmospheric Chemistry and Physics*, **13**, 2063-2090.

736 Zardi, D., and C. D. Whiteman, 2013: Diurnal Mountain Wind Systems. *Mountain Weather*  
737 *Research and Forecasting: Recent Progress and Current Challenges*, F. K. Chow, S. F. J. De  
738 Wekker, and B. J. Snyder, Eds., Springer Netherlands, 35-119.

739 Zhang, X., J. H. Helsdon, and R. D. Farley, 2003: Numerical modeling of lightning-produced NO<sub>x</sub>  
740 using an explicit lightning scheme: 1. Two-dimensional simulation as a “proof of concept”.  
741 *Journal of Geophysical Research: Atmospheres*, **108**.

742 Zhang, X., X. Chen, and X. Zhang, 2018: The impact of exposure to air pollution on cognitive  
743 performance. *Proceedings of the National Academy of Sciences*, **115**, 9193-9197.

744 Zhong, S. Y., C. D. Whiteman, and X. D. Bian, 2004: Diurnal evolution of three-dimensional wind  
745 and temperature structure in California's Central Valley. *Journal of Applied Meteorology*, **43**,  
746 1679-1699.

747 Ziemke, J. R., B. N. Chandra, L. Duncan, P. K. Froidevaux, P. K. Bhartia, P. F. Levelt, and J. W.  
748 Waters, 2006: Tropospheric ozone determined from Aura OMI and MLS: Evaluation of  
749 measurements and comparison with the global modeling initiative's chemical transport  
750 model. *Journal of Geophysical Research*, **111**.

751

752 **Tables**753 **Observational Overview Table:**

<b>Bodega Bay, Ozonesonde Site, (38.319N, -123.072W), San José State University</b>		
<b>Parameters Observed</b>	<b>Method</b>	<b>Date Interval</b>
O <sub>3</sub>	Electrochemical Concentration Cell (ECC)	6 days/week May 16 to August 16
T, RH	bead thermistor & capacitance hygrometer	
winds	GPS tracking	
<b>Half Moon Bay, Ozonesonde Site, (37.505N, -122.484W), San José State University</b>		
<b>Parameters Observed</b>	<b>Method</b>	<b>Date Interval</b>
O <sub>3</sub>	Electrochemical Concentration Cell (ECC)	6 days/week July 24 to August 17
T, RH	bead thermistor & capacitance hygrometer	
winds	GPS tracking	
<b>Chews Ridge, Mountain Inflow Monitoring Site, (36.306N, -121.567W), University of California Davis/Monterey Institute for Research in Astronomy</b>		
<b>Parameters Observed</b>	<b>Method</b>	<b>Date Interval</b>
O <sub>3</sub>	UV-Absorption (2B-Tech)	May 1 to August 31
NO/NO <sub>x</sub>	Chemiluminescence/Photolysis (TECO w Mo convertor)	
T, RH, Wind speed/direction	Davis Instruments	
<b>Mooney Aircraft, University of California Davis/Scientific Aviation, Inc.</b>		
<b>Parameters Observed</b>	<b>Method</b>	<b>Date Interval</b>
O <sub>3</sub>	UV-Absorption (2B-Tech)	June 2-4, June 28, July 24-26, July 27-29, August 4-6, August 12-18
NO/NO <sub>x</sub>	Chemiluminescence/Photolysis (EcoPhysics/Air Quality Design, Inc.)	
CH <sub>4</sub> /CO <sub>2</sub> /H <sub>2</sub> O	Picarro CaRDS	
T, RH	Vaisala Instruments	
Horizontal Winds	In-house dual GPS (Hemisphere)	
<b>AJAX, NASA Ames Research Center</b>		
<b>Parameters Observed</b>	<b>Method</b>	<b>Date Interval</b>
O <sub>3</sub>	UV-Absorption (2B-Tech model 205)	May 12, May 19,
CH <sub>4</sub> /CO <sub>2</sub> /H <sub>2</sub> O	IR Cavity Ringdown Spectroscopy (Picarro model G2301-m)	June 3, June 15,
3-D winds, P, T	NASA Ames MMM package	June 23, July 6,

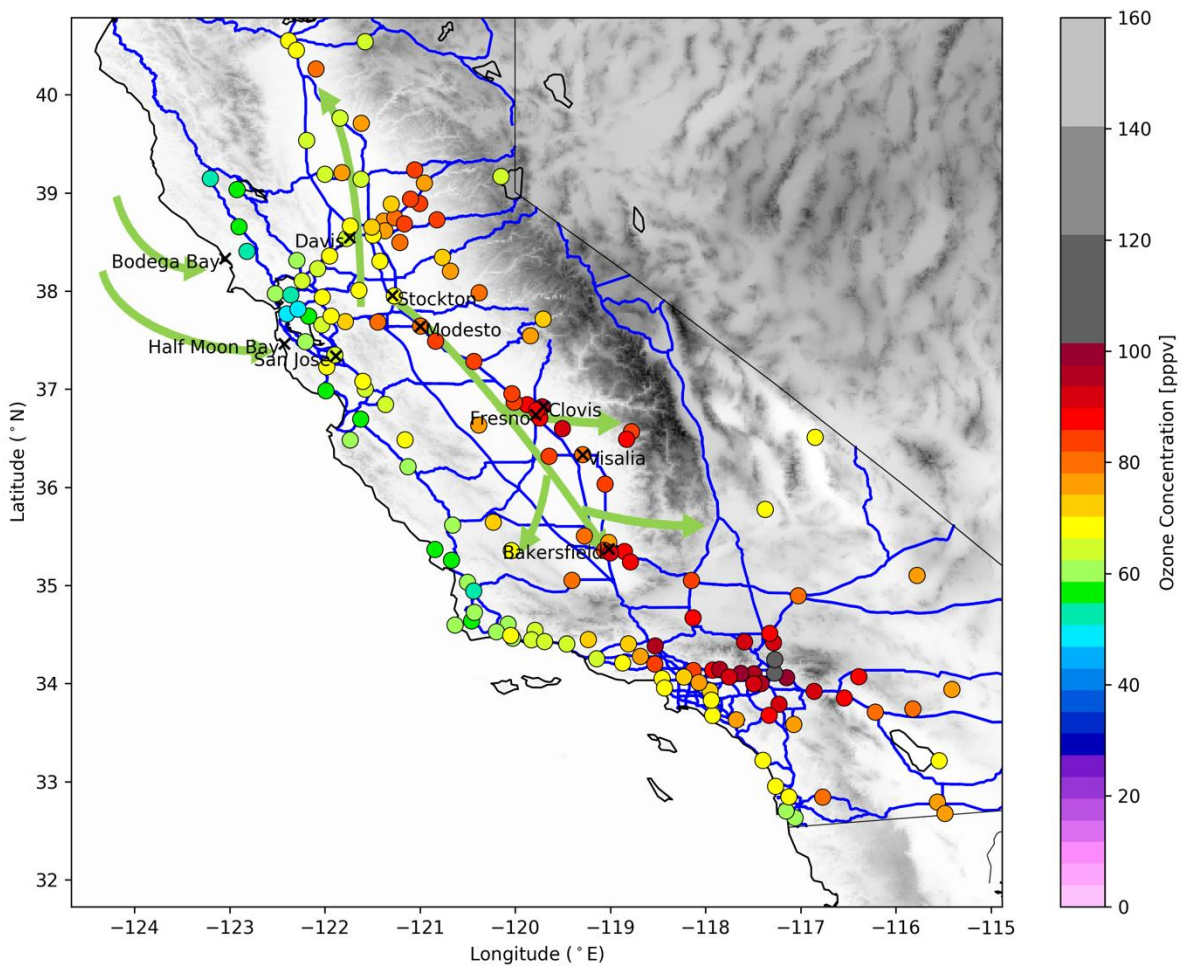


		July 21, & July 28 2016
HCHO	non-resonant laser-induced fluorescence	May 12, June 15, June 23, July 21, July 28
<b>TOPAZ ozone lidar, NOAA Earth System Research Laboratory</b>		
<b>Parameters Observed</b>	<b>Method</b>	<b>Date Interval</b>
O <sub>3</sub> , Aerosol backscatter profiles	Differential Absorption Lidar (DIAL)	May 27 – June 18, July 18- August 7
O <sub>3</sub>	UV-Absorption (2B-Tech model 205)	May 27 – August 8
T, p, RH, wind speed and direction	Airmar 150WX weather station	May 27 – August 8

754

755 **Figures**

756



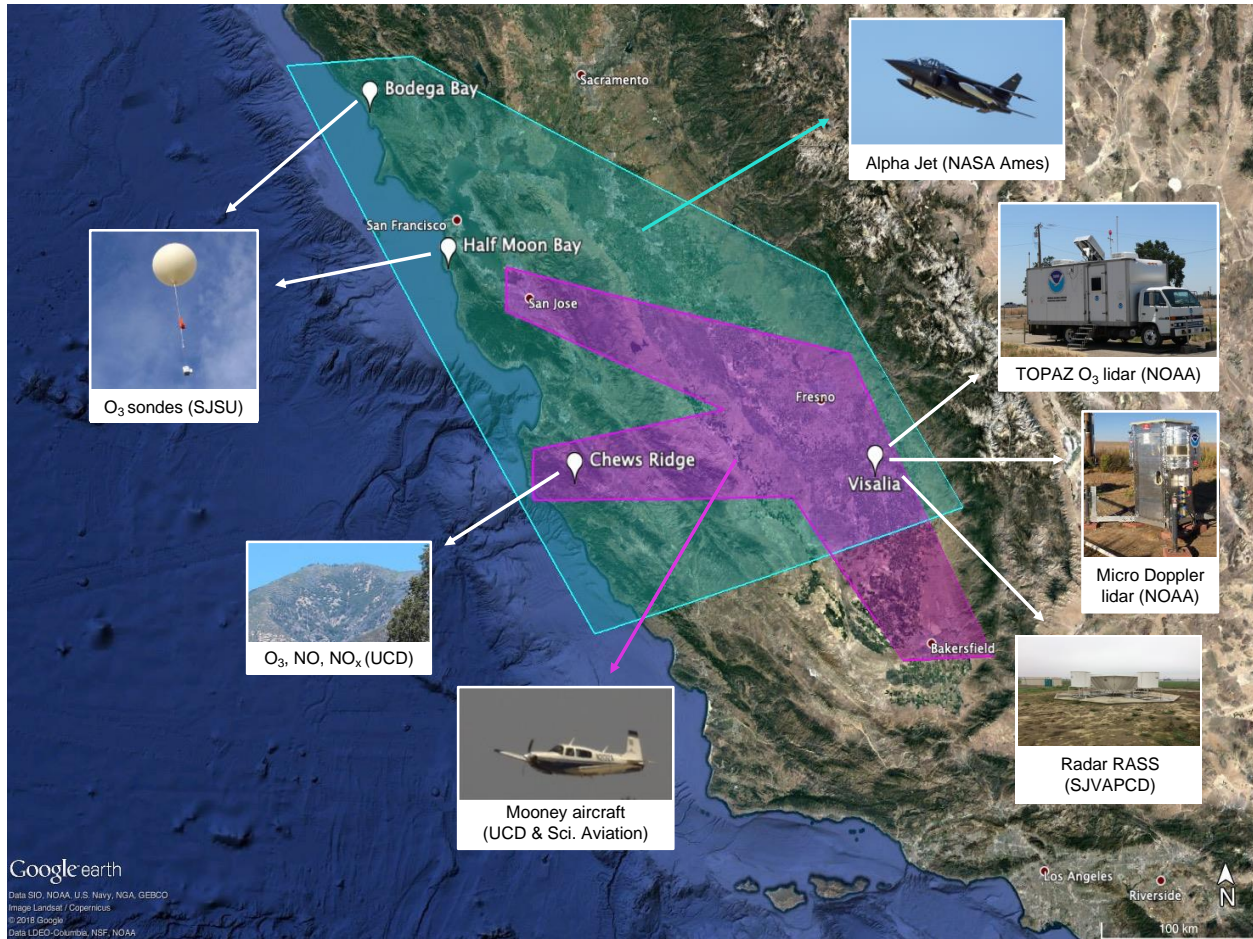
757

758 Figure 1. 2016 ozone design values (ODV) across the state of California from the CARB surface air  
759 quality network. The ODV is defined as the three year running mean of each year's fourth highest  
760 maximum daily 8-hr average (MDA8) ozone concentration. Thin blue lines represent major  
761 highways, and thick green arrows show the typical daytime air flow near the surface during the  
762 warm season.

763

764

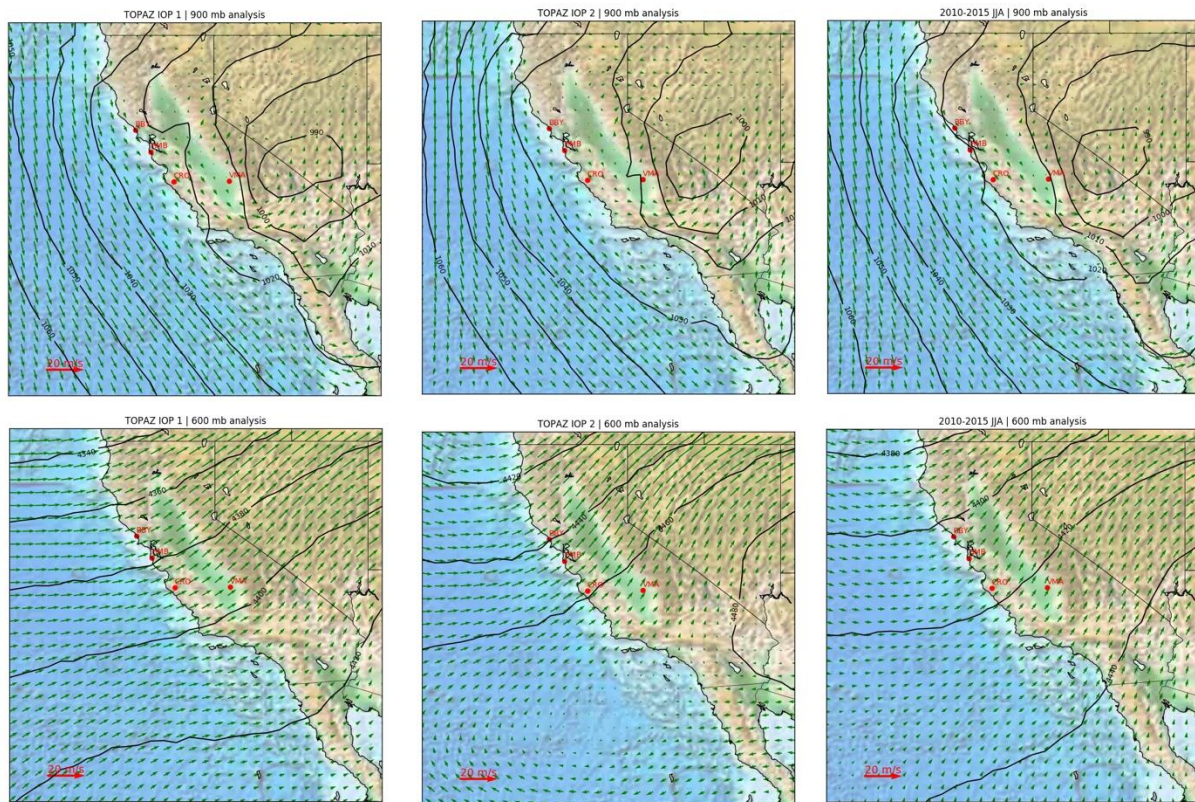
765



766 Figure 2. Overview of CABOTS study domain and measurement platforms ranging from daily  
767 ozonesondes launched at the two coastal sites (Bodega Bay & Half Moon Bay) to the NOAA TOPAZ  
768 lidar in Visalia. The green and purple polygons represent the approximate domains surveyed by  
769 the NASA Alpha jet and Scientific Aviation, Inc. Mooney aircraft, respectively.

770

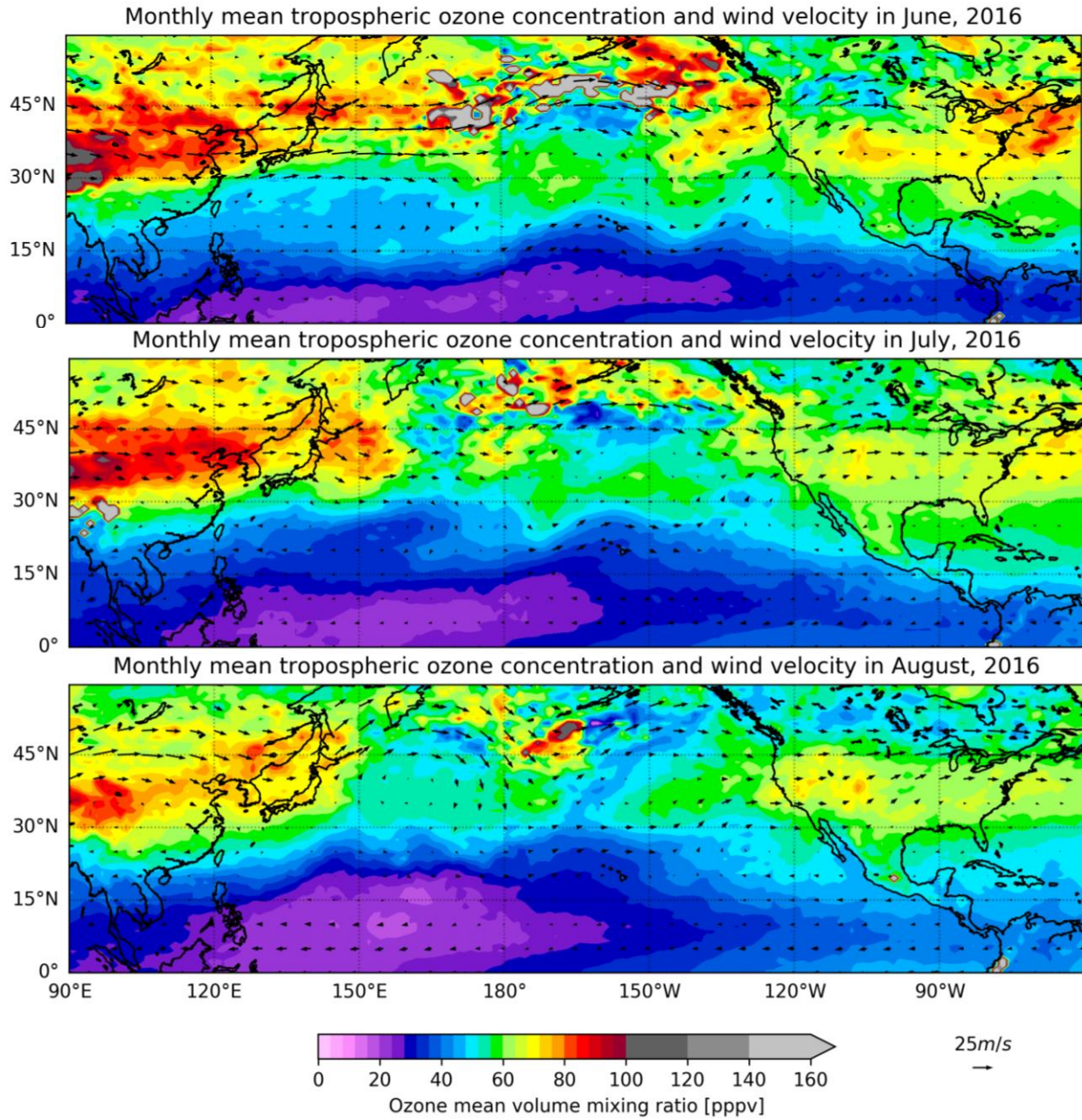
771



772

773 Figure 3. Geopotential heights for CABOTS at 900 hPa (top row) and 600 hPa (bottom row) for  
774 IOP1 (left), IOP2 (middle), and climatological average for June – August 2010-2015 (right). The  
775 two pressures are near the altitudes of maximum correlation found between O<sub>3</sub> observations at  
776 Bodega Bay (BBY) and Visalia Municipal Airport (VMA).

777

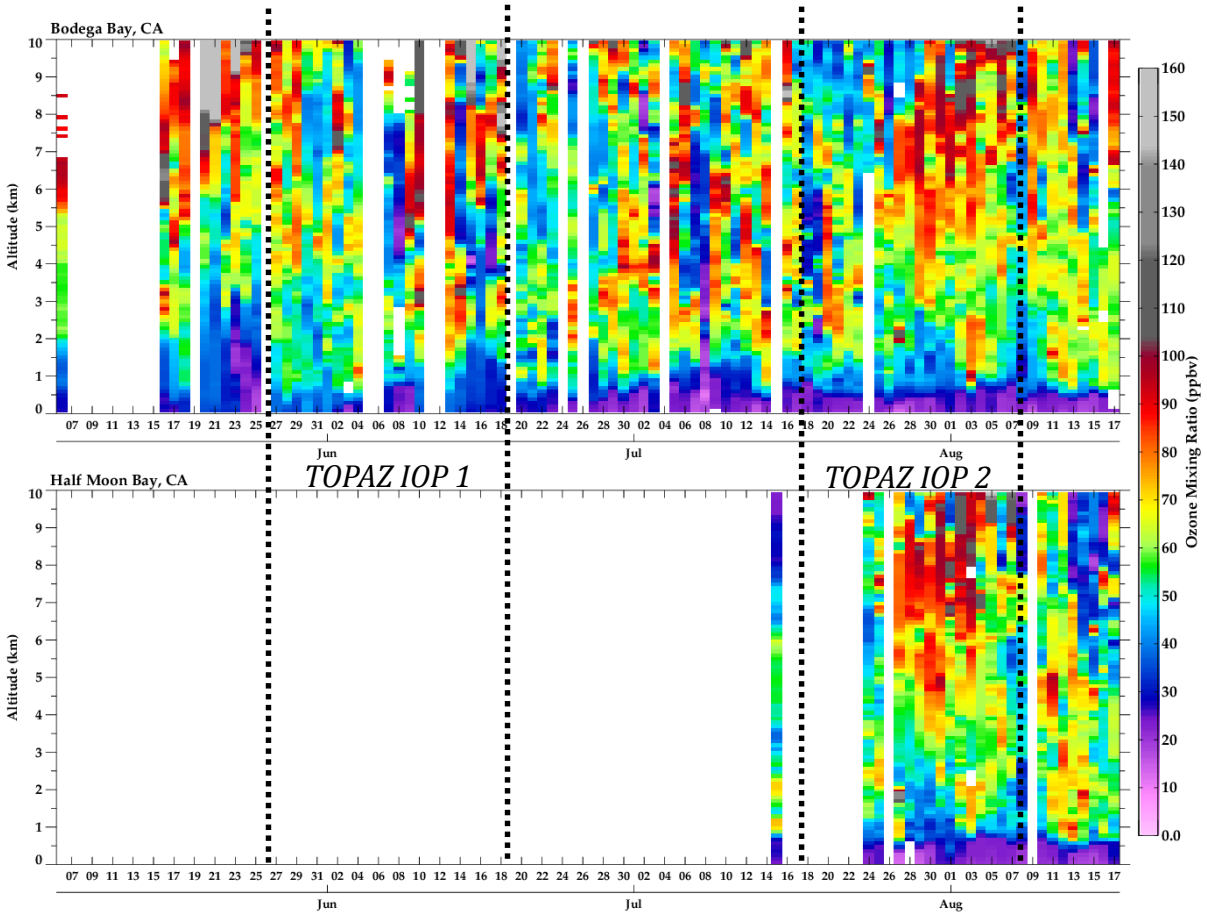


778

779 Figure 4. NASA Goddard tropospheric column O<sub>3</sub> product from Aura OMI/MLS and the NCEP

780 Reanalysis winds at 300 hPa for the summer months of the CABOTS project.

781



782

783

784 Figure 5. Ozonesonde profiles measured at Bodega Bay and Half Moon Bay during CABOTS

785 (vertical dashed lines indicate TOPAZ IOPs).

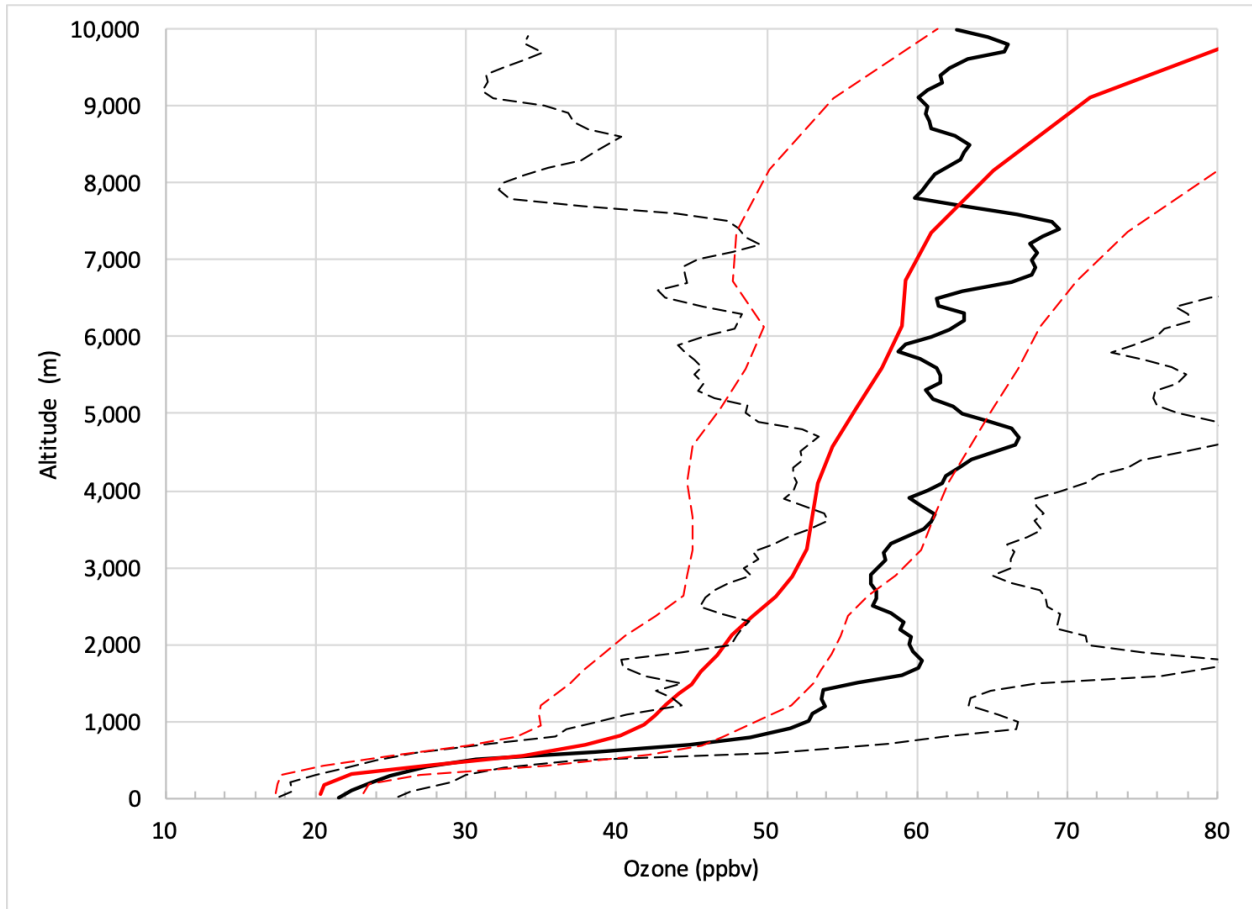
786

787

788

789

790



791

792

793 Figure 6. Mean (solid line) and  $\pm 1$  standard deviation (dashed lines) of the observed ozone (black)

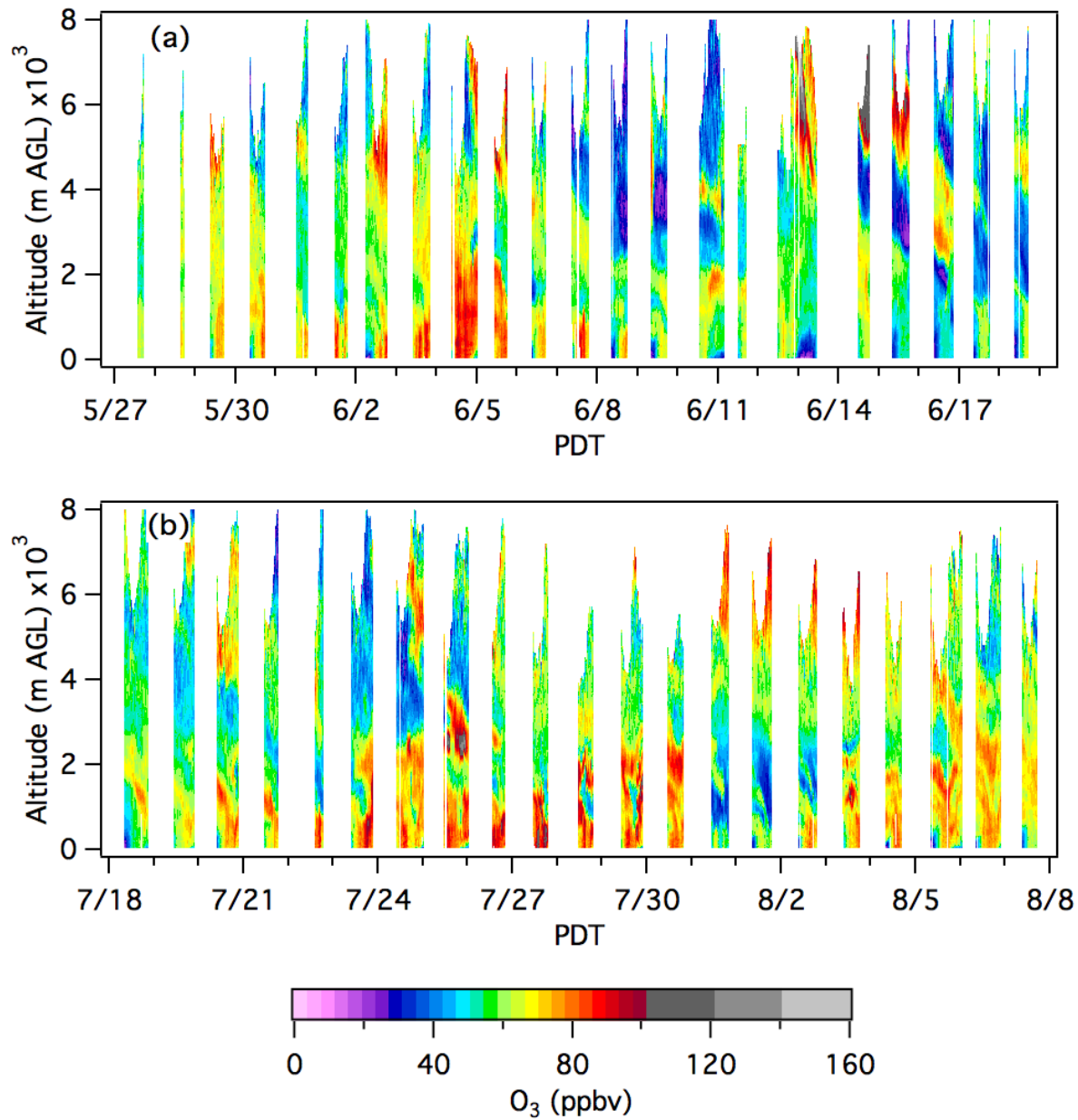
794 and the model ozone from MOZART (red) above the Half Moon Bay site. The comparison is for

795 24 days between mid-July and mid-August 2016.

796

797

798



799

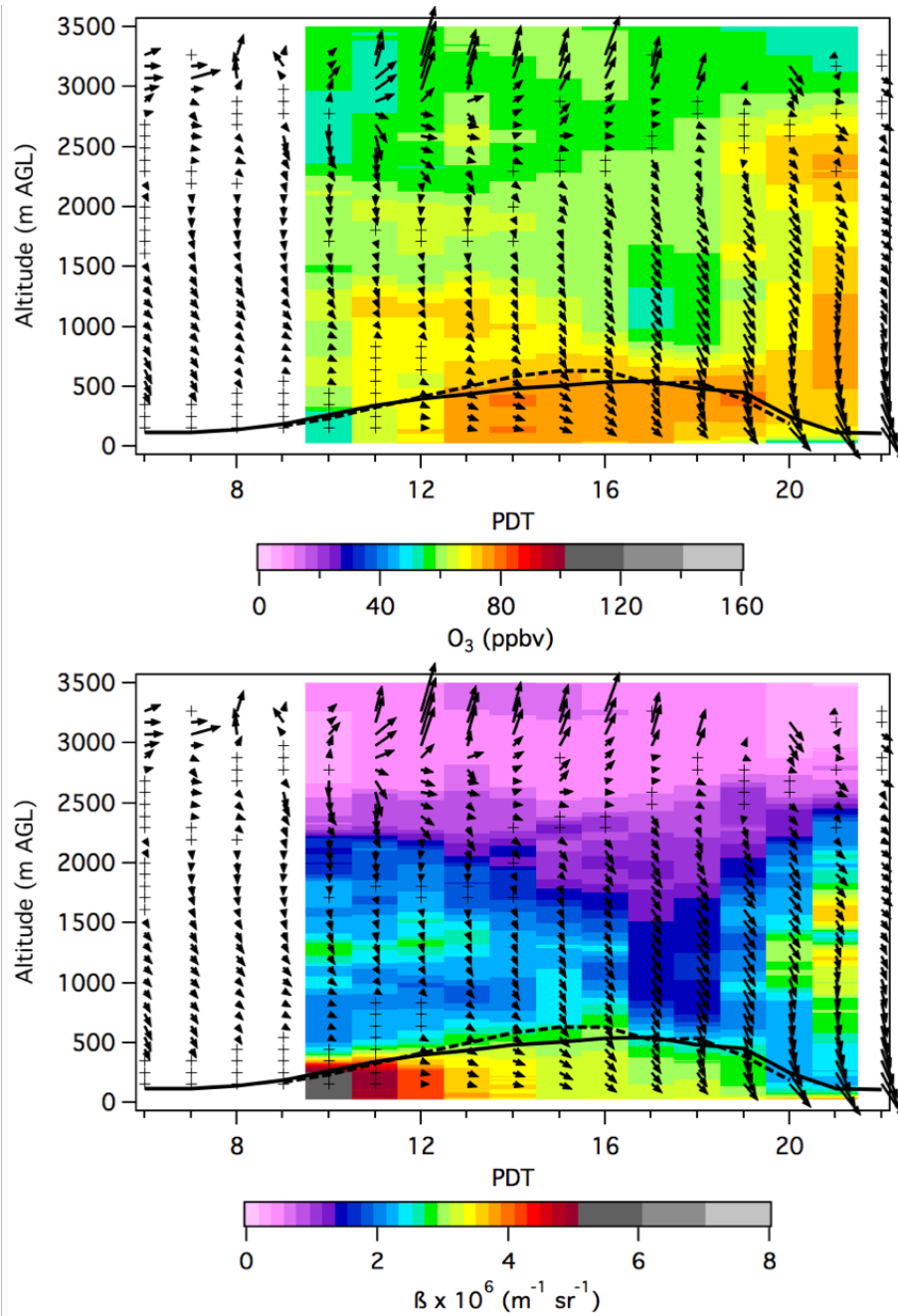
800 Figure 7. TOPAZ O<sub>3</sub> lidar profiles for (a) IOP1 and (b) IOP2.

801



802

803



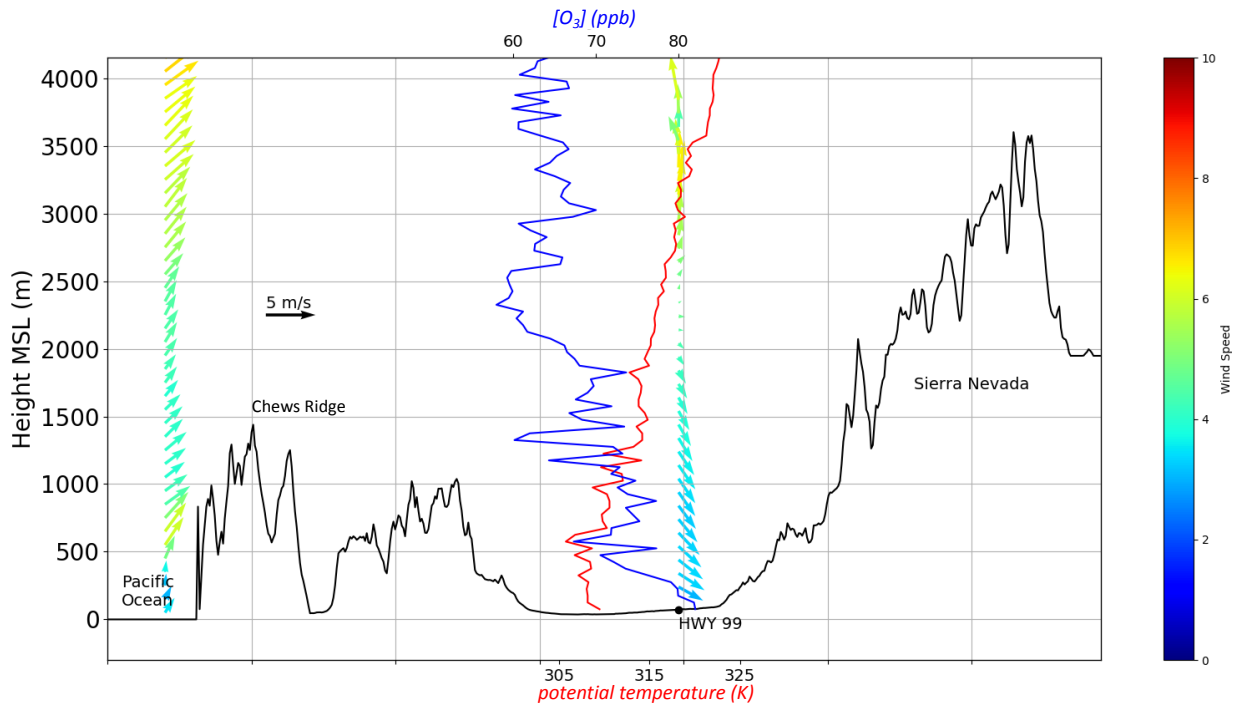
804

805 Figure 8. Mean diurnal profiles of TOPAZ ozone (top) and backscatter (bottom), along with winds

806 from the co-located SJVAPCD radar profiler and RASS during the second CABOTS IOP. The black

807 lines show the ABL height inferred from the RASS temperature profiles (solid) and a co-located  
808 NOAA Doppler lidar (dashed).

809



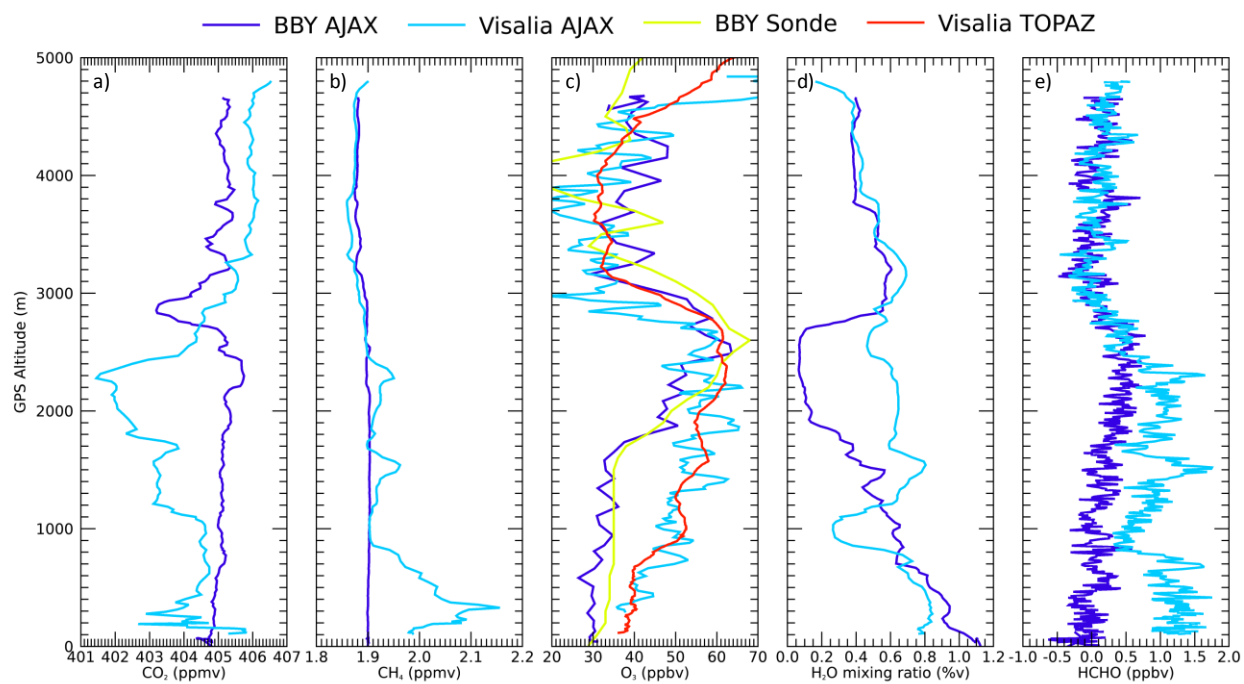
810

811 Figure 9. Cross section of SJV through the Chews Ridge site passing across CA Hwy 99 between  
812 Madera & Merced (approximately 100 km north of Visalia). Vector average winds as a function  
813 of height and mean scalar wind speed (colors), shown with respect to north directed straight up,  
814 from the coastal wind profile observed by sondes at Half Moon Bay (approximately 100 km north  
815 of Chews Ridge), and at Visalia by the RASS for 12:00-16:00 PST July-August 2016. Ozone (blue)  
816 and potential temperature (red) are averages from the afternoon Mooney aircraft flights profiling  
817 throughout the region.

818

819

820

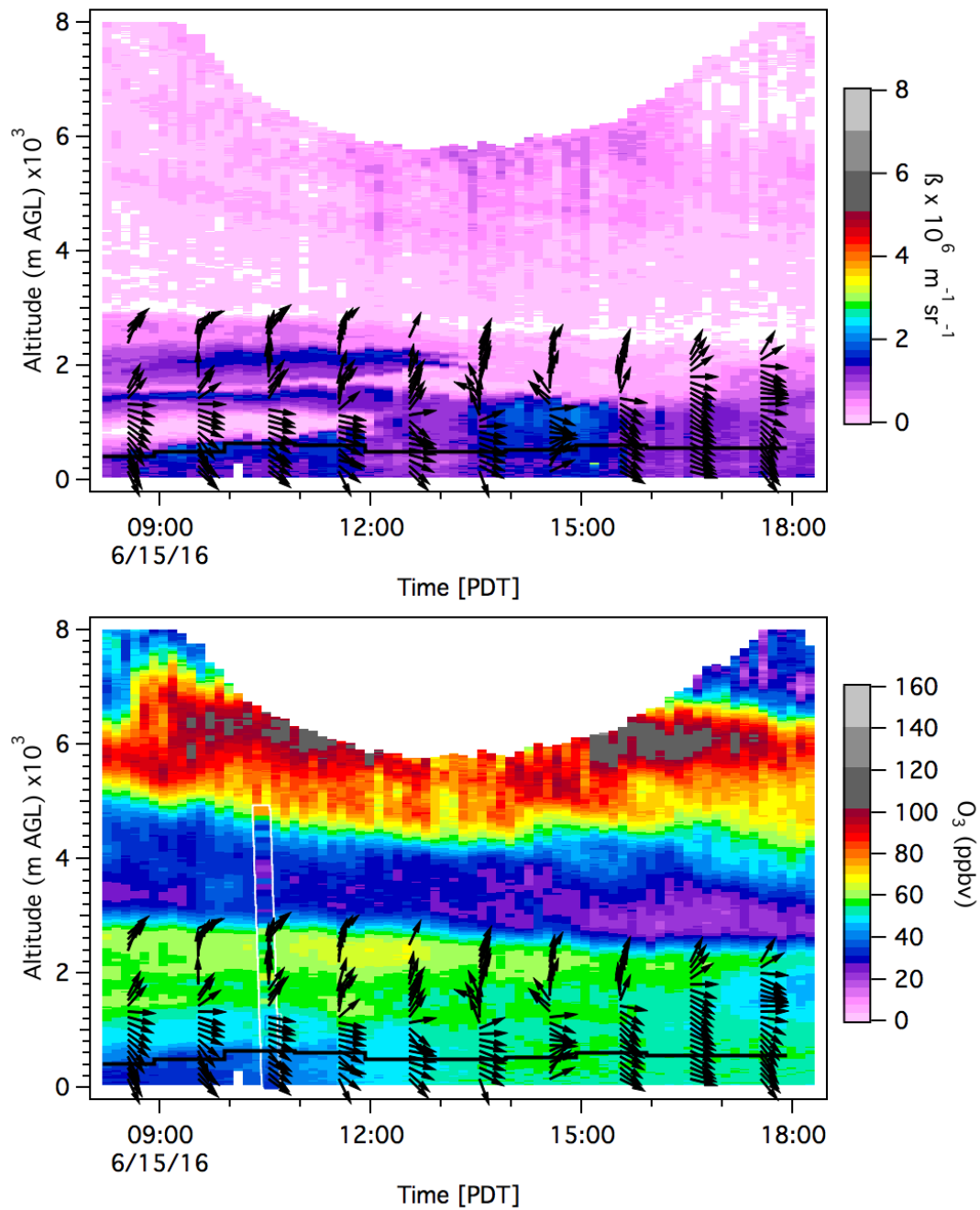


821

822 Figure 10. June 15, 2016 AJAX profiles taken at BBY and VMA (dark and light blue, respectively)  
823 of (a) CO<sub>2</sub>, (b) methane, (c) ozone, (d) water vapor, and (e) formaldehyde. Aircraft profiles were  
824 measured at 10:00 PDT at Bodega Bay and half an hour later at Visalia. The profiles of ozone  
825 measured by the ozonesondes at Bodega Bay (yellow) and from the TOPAZ lidar at Visalia (red)  
826 are superimposed in (c) for comparison.

827

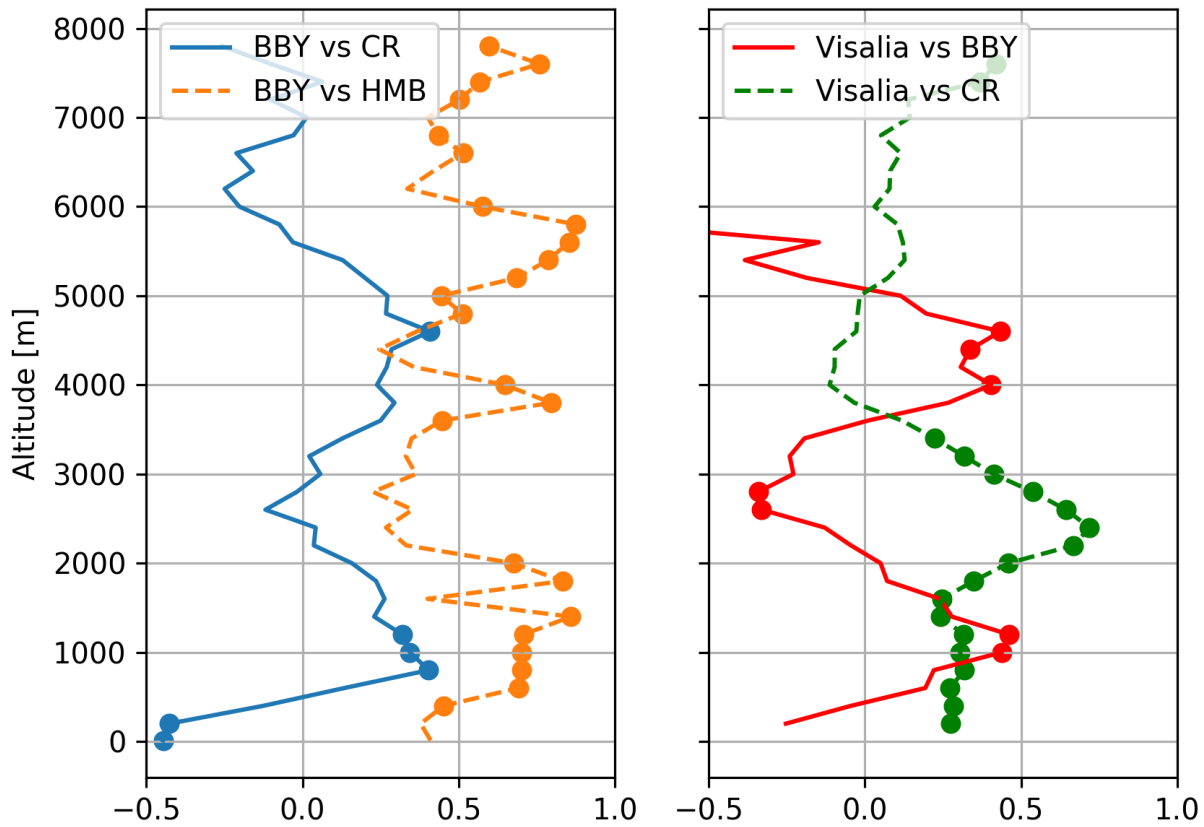
828



830 Figure 11. Time-height curtain plots of the TOPAZ aerosol backscatter (top) and ozone (bottom)  
 831 above the VMA with the co-located profiler winds and RASS boundary layer height. The AJAX  
 832 ozone profile above the VMA is superimposed on the ozone plot (~10:30-40 PDT).

833

834



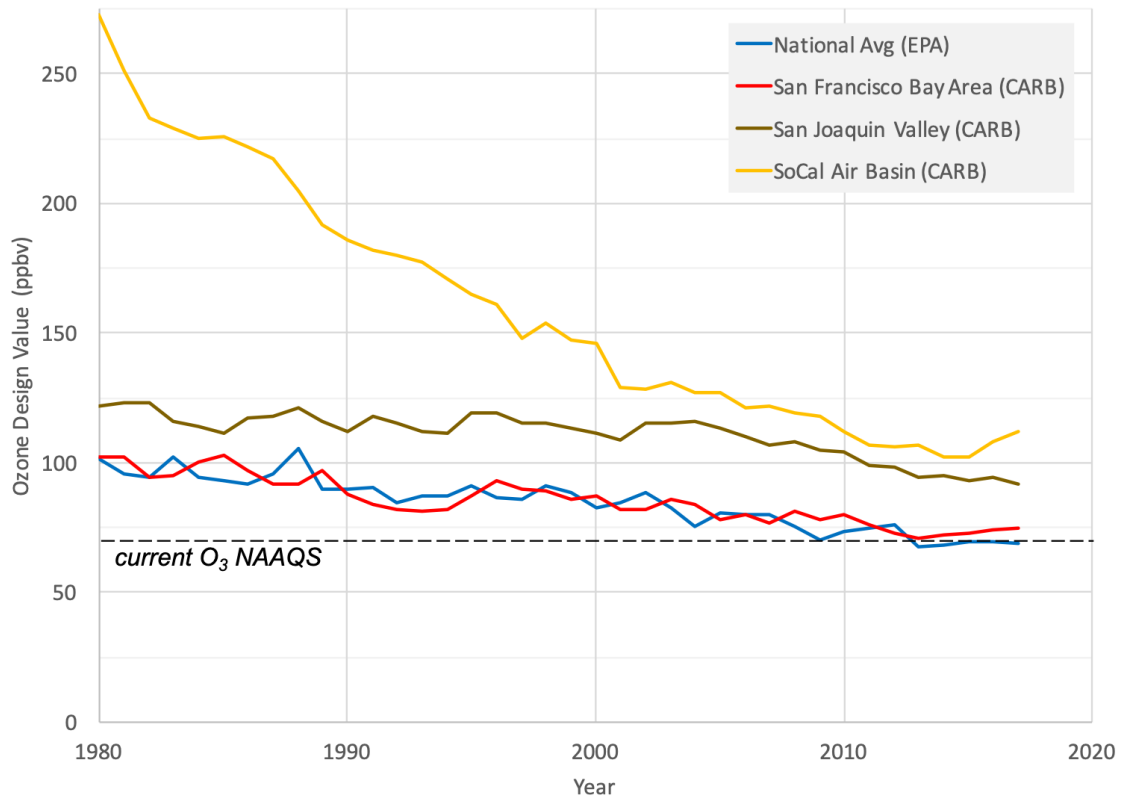
835

836 Figure 12. (Left) Correlation coefficients of Bodega Bay ozonesondes observations with  
837 coincident Chews Ridge surface ozone at 1.5 km (blue line), and Half Moon Bay ozonesonde  
838 measurements (orange dashed line). (Right) Correlations of TOPAZ lidar data with Bodega Bay  
839 ozonesondes (red line) and Chews Ridge surface (green line). Circles represent correlations with  
840 p-values < 0.05.

841

842

843



844

845 Figure SB1. The decadal trends in ozone design values from three different air basins in  
846 California compared to the national average and the current National Ambient Air Quality  
847 Standard (NAAQS.)

848

849

850



851

852 Figure SB2. Three views of the Soberanes Fire taken during CABOTS. (top left) View from Scientific  
853 Aviation, Inc. Mooney aircraft looking northward from Chews Ridge. (bottom left) View towards  
854 the southwest from the Oliver Observing Station on Chews Ridge (photo credit: Chris Reed,  
855 observatory caretaker). (right) MODIS satellite image of the fire from July 26, 2016  
856 (<https://earthobservatory.nasa.gov/images/88483/wildfire-along-the-california-coast>).

857

858

859

Final responses to second round of reviews for “The California Baseline Ozone Transport Study (CABOTS)” submission to BAMS

2nd Review of "The California Baseline Ozone Transport Study (CABOTS)" by Faloon et al.  
MS Number: BAMS-D-18-0302

Summary:

I originally recommended that this paper be rejected, largely based on my question whether BAMS is the appropriate journal for this paper. Since my recommendation was not followed, I assume that the editor does find the paper appropriate. Further, the paper has been shortened and the discussion improved. I recommend publication after the following minor issues are addressed.

Minor issues:

1) Lines 156-157 mention “... near-daily ozonesonde profiles collected at one site on the coast and ozone ...” but the figure under discussion shows two sites. I suggest that the discussion in this sentence be clarified.

*Changed to, “The core measurements included near-daily ozonesonde profiles collected at two sites along the coast and an ozone lidar data set collected in Visalia, a city of nearly 140,000 residents located deep within the San Joaquin Valley, approximately 60 km southeast of Fresno.”*

2) Line 233: “comprised” would be better replaced by “composed”.

*Changed to “composed”.*

3) Lines 297-300: In the discussion of Figure 6, the authors may wish to note that the observations show only a small mean vertical ozone gradient between 2 and 10 km (<1 ppb/km) while the model shows a significantly stronger gradient (~3.3 ppb/km). The authors may also wish to note that the median of the observations approaches 60 ppb in the 1.5 to 3 km altitude range, which is only 10 ppb below the current NAAQS. The + 1 std. dev is close to the NAAQS, but the NAAQS represents above a + 2 std. dev. value. Hence, if the air between 1.5 and 3 km were transported to the surface of the Central Valley without dilution, O<sub>3</sub> above the NAAQS would occasionally be observed at surface sites.

*Thank you for the additional comments on the model, but based on some critical comments about the MOZART model that we received from another technical reviewer of this manuscript, we feel that it would not be helpful to include more specific analysis of the model results here. Moreover, it is our opinion that transport of air aloft into the boundary layer without mixing is not a physically relevant scenario, not to mention that in order to violate the NAAQS it would have to persist for at least 8 hours. But considering your points more carefully, we have decided to include a sentence to draw attention to the fact that elevated surface sites may experience these higher ozone levels even in the absence of contributions from local sources. Consequently,*



*we have added a sentence to that paragraph that reads, “Furthermore, in agreement with the findings presented in Figure 6 of frequent ozone concentrations well above 60-70 ppb (mean + 1 standard deviation) at 1.5 km altitudes and above, an analysis of the ozone time series collected at Chews Ridge from 2012-2014 determined that the ODV for this remote site located in a National Forest in the coastal mountains was 70.5 ppbv, technically in violation of the NAAQS.”*

4) Lines 314-315: This description is confusing, at least to this chemist. Northwesterly winds have vectors that point to the bottom and right, so perhaps the top represents south, and the right side represents west? Please clarify.

*It is meteorological convention to name the wind based on the direction from which it blows. This is opposite to the oceanographic convention of naming a current by the direction it is moving toward, so confusion in the Earth Sciences is easy. The wind vectors under consideration are pointing to the right and then bottom/right, so they are blowing from the west(erly) and northwest(erly) directions. We have added the following clause for absolute clarity, “The wind vectors show the horizontal wind direction with the top of the plot representing north and the right side east (arrows that point to the right in the figure therefore represent westerly winds.)*

5) Line 329: O<sub>3</sub> depletion overnight in a shallow nocturnal boundary layer does not necessarily require nitrate production. NO<sub>2</sub> formation, surface deposition, and downslope flow of cleaner air may be enough to explain this?

*Yes, line 329 states that O<sub>3</sub> depletion is occurring predominantly due to nitrate production **and** dry deposition, both of which were estimated in the Caputi et al. (2019) reference wherein we attempted to quantify all these terms overnight (including advection) based on a simplified odd oxygen (O<sub>3</sub>+NO<sub>2</sub>) budget so as not to include titration. While not covered in this work, we measured ~2 ppb NO and ~7 ppb NO<sub>2</sub> in the afternoons in this region, so we expect the significant lowering of O<sub>3</sub> near the surface in the dark to be due mostly to reaction with NO<sub>2</sub>, not simply titration. We find the average loss of O<sub>x</sub> overnight due to nitrate production to be -2.7 ppb/h, compared with -1.2 ppb/h due to dry deposition and -0.2 ppb/h for horizontal advection in addition to +2.8 ppb/h from vertical mixing.) We were hoping that readers interested in the overnight ozone chemistry would read our further analysis presented in Caputi et al. (2019).*

6) Line 330-333: The prevalence of elevated ozone (>70 ppb, orange colors) between 500 – 2,500 m in these average profiles of Figure 8 is cited as evidence that ABL air is lofted into the buffer layer above due to daytime slope flow along the eastern flank of the valley during its up-valley progression to the southeast. Is this really correct? Figure 6 shows that mean ozone coming ashore between 500 and 2500 m can average 60 ppb. Very little additional O<sub>3</sub> from ABL air would be required to reach 70 ppb. Please discuss how persuasive is the evidence provided by these relatively small enhancements in O<sub>3</sub>.

*First, the average of the profile in the layer between 500 – 2,500 m in Figure 6 is much closer to 50 ppbv, which leads to enhancements of ozone within the valley at those altitudes of over 20 ppb, which is indeed significant. Second, enhancements over the baseline in the much deeper*

*buffer layer are proportionally larger than a mere additive ppb, given that the ABL has only about one-third of the mass of the buffer layer. Third, we go to greater lengths to support this assertion in the discussion surrounding figure 10, which clearly shows discrete, elevated layers of other corroborating scalars above the valley within the BuL. And finally, this effect is well established in the literature, including references that we have cited (Leukauf et al., 2016; Fast et al., 2012) and others we did not have the space to cite (Rotach et al., 2015; Serafin et al., 2018). Nevertheless, we have added a sentence to draw attention to the continuing analysis in the manuscript, “Further evidence of this slope venting is presented for other scalars in the discussion surrounding Figure 10 that follows.”*

7) Line 341-342: (Same comment as 4 above.)

*Hopefully the added comment in lines 314-315 help clarify.*

8) Line 392-393: Low aerosol and high ozone might indicate stratospheric source rather than Asian? Please clarify.

*The sentence on lines 392-393 states that the low aerosol and high ozone are **consistent** with transported Asian pollution. Looking back at the original submission’s Figure 13, it illustrates the AJAX flight data from June 15, the same day being discussed here in the current Figure 11. That figure, which was eliminated at the suggestion of reviewers, showed that the layer near 5 km above Visalia showed signs of elevated levels of CO<sub>2</sub>, HCHO, and CH<sub>4</sub>, thus providing further evidence that its origin is not the stratosphere. We have added a statement to the following sentence to make this clear in the new draft, “The superimposed AJAX profile in Figure 11 shows that the aircraft sampled the very bottom of the transported pollution layer (not shown here, but exhibiting enhanced CO<sub>2</sub>, HCHO, and CH<sub>4</sub>) before descending into the clean layer.”*

9) Line 411: “... just below 1 km ...” is better described as “... 0.8 to 1.2 km ...”

*Changed.*